

Exendin-4 Induces Cytotoxic Autophagy in Two Ovarian Cancer Cell Lines through Inhibition of Mtorc1 Mediated by Activation of AMPK and Suppression of Akt

(Exendin-4 / ovarian cancer / autophagy / AMPK / PI3K / Akt / mTORC1)

R. M. BADI^{1,2}, E. F. KHALEEL^{1,3}, M. H. EL-BIDAWY^{4,3}, H. H. SATTI^{5,6},
D. G. MOSTAFA^{1,7}

¹Department of Physiology, ⁵Department of Pathology, College of Medicine, King Khalid University, Abha, Saudi Arabia

²Department of Physiology, ⁶Department of Pathology, Faculty of Medicine, University of Khartoum, Khartoum, Sudan

³Department of Medical Physiology, Faculty of Medicine, Cairo University, Cairo, Egypt

⁴Department of BMS, Division of Physiology, College of Medicine, Prince Sattam Ibn Abdulaziz University, Al-Kharj, Saudi Arabia

⁷Department of Medical Physiology, Faculty of Medicine, Assiut University, Assiut, Egypt

Abstract. Activation of autophagy suppresses ovarian cancer (OC). This *in vitro* study investigated whether the anti-tumour effect of exendin-4 against OC involves modulation of autophagy and figured out the possible mechanisms of action. SKOV-3 and OVCAR-3 cells (1×10^5 /ml) were cultured in DMEM medium and treated with exendin-4 in the presence or absence of chloroquine (CQ), an autophagy inhibitor. In some cases, cells were also treated with exendin-4 with or without pre-treatment with compound C (CC), an AMPK inhibitor, or insulin-like growth factor (IGF-1), a PI3K/Akt activator. Exendin-4 increased expression of beclin-1 and LC3I/II, suppressed expression of p62, reduced cell survival, migration, and invasion, and increased cell apoptosis and LDH re-

lease in both SKOV-3 and OVCAR-3 cells. Besides, exendin-4 reduced phosphorylation of mTORC1, 6SK, 4E-BP1, and Akt but increased phosphorylation of AMPK in both cell lines. These effects were associated with down-regulation of Bcl-2, suppression of nuclear phosphorylation of NF- κ B p65, and increased expression of Bax and cleaved caspases 3/8. Chloroquine completely prevented the inhibitory effects of exendin-4 on the cell survival, Bcl-2, NF- κ B, and cell invasiveness and abolished its stimulation of cell apoptosis and LDH release. Moreover, only the combined treatment with IGF-1 and CC completely abolished the observed effect of exendin-4 on the expression of beclin-1, LC3I/II, p62, as well as on cell survival, apoptosis, and LDH release. Exendin-4 exhib-

Received May 18, 2020. Accepted October 20, 2020.

This work was fully funded by the Deanship of Scientific Research, King Khalid University through the General Research Projects Funding Program (Grant number 127/40).

Corresponding author: Rehab M. Badi, Department of Medical Physiology, King Khalid University, Abha, Saudi Arabia. P.O. Box 3340, King Khalid University, ElSamer, Abha, 61421 Saudi Arabia; e-mail: rehabadi@hotmail.com

Abbreviations: 4E-BP1 – eukaryotic translation initiation factor 4E-binding protein 1, Akt – protein kinase B, AMPK – adenosine monophosphate-activated protein kinase, Bcl-2 – B-cell lymphoma 2, BrdU – bromo-2'-deoxyuridine, CC – compound C, CCK-8 – cell counting kit-8, CQ – chloroquine, DMEM – Dulbecco's modified Eagle's medium, DMSO – dimethyl sulphoxide, ERK – extracellular signal-regulated kinases, FB – foetal bovine serum,

GLP-1 – glucagon-like peptide 1, GSH – reduced glutathione, HepG2 – liver hepatocellular carcinoma cell line, LC3 – microtubule-associated protein 1A/1B-light chain 3, LDH – lactate dehydrogenase, LKB1 – liver kinase B1, MAPK – mitogen-activated protein kinases, mTOR – mammalian target of rapamycin, NAD⁺ – nicotinamide adenine dinucleotide, NADPH – nicotinamide adenine dinucleotide phosphate, NF- κ B – Nuclear factor κ -light-chain-enhancer of activated B cells, OC – OVCAR-3 – ovarian carcinoma cell line, p-4E-BP1 – phosphorylated eukaryotic translation initiation factor 4E-binding protein 1, p-Akt – phosphorylated protein kinase B, p-AMPK – phosphorylated adenosine monophosphate-activated protein kinase, PBS – phosphate-buffered saline, PI3K – phosphatidylinositol-3-kinase, POD – BrdU-peroxidase, p-S6K1 – phosphorylated ribosomal protein S6 kinase β -1, S6K1 – ribosomal protein S6 kinase β -1, SIRT 1 – silent inflammatory regulator 1, SKOV-3 – ovarian cancer cell.

its a potent anti-tumour cytotoxic effect in SKOV-3 and OVCAR-3 cells by activating the markers of autophagy, mediated by activation of AMPK and inhibition of Akt.

Introduction

Ovarian carcinoma (OC) is the most lethal gynaecological malignancy, with a 5-year survival rate of less than 30 % (Vaughan et al., 2011). Dysregulation of autophagy is considered as a primary factor in the initiation, progression, and metastasis of OC, and in the development of drug resistance (Zhan et al., 2016). Targeting proteins and signalling pathways involved in autophagy are currently under focus to improve the outcome of OC (Peracchio et al., 2012; Tang et al., 2019).

Autophagy is an evolutionarily conserved self-digestion pathway that maintains cellular homeostasis and metabolic adaptation through recycling macromolecules, damaged cellular components, and organelles (Mizushima et al., 2008). In normal cells, autophagy exists at basal levels that can be up-regulated in response to stressful stimuli such as starvation, oxidative stress, endoplasmic reticulum stress, and infections (Ylä-Anttila et al., 2009; Ding et al., 2014). Serine/threonine kinase mammalian target of rapamycin (mTOR) is the primary inhibitor of autophagy in most cells. mTOR is under the regulation of two major signalling pathways: phosphatidylinositol-3-kinase (PI3K)/AKT pathway, and liver kinase B1 (LKB1)/adenosine monophosphate-activated protein kinase (AMPK) pathway (Zhan et al., 2016). The PI3K/Akt pathway activates mTOR and inhibits autophagy, while LKB1/AMPK activates autophagy through inhibiting mTOR (Vijayakumar and Cho, 2019). The regulation of autophagy is also interconnected with other signalling pathways that are involved in cell proliferation and apoptosis such as the Ras/MAP and p38 MAPK /JNK pathways (Zhan et al., 2016; Vijayakumar and Cho, 2019).

In OC, autophagy can either be a tumour promoter or suppressor (Liu and Ryan, 2012; Yun and Lee, 2018). Whether autophagy promotes tumour progression or regression depends on several factors including the stage of the disease, nutrient deficiency or hypoxia in the tumour microenvironment, chemo-resistance, and contribution of various signalling pathways (Liu and Ryan, 2012; Yun and Lee, 2018). In general, down-regulation of autophagy promoted the development of OC (Shen et al., 2008; Correa et al., 2015; Zhan et al., 2016). Inhibition of the PI3K/Akt/mTOR signalling pathway restricted OC development by activating autophagy (Lu et al., 2014; Bai et al., 2015; Zi et al., 2015). Nevertheless, in the context of chemotherapy treatment for OC, activation of autophagy contributed to the development of chemotherapy resistance (Morgan et al., 2014; Sun et al., 2015; Tang et al., 2019). Researchers found that the activation of autophagy rendered OC more resistant to chemotherapy, whereas its inhibition by pharmacological agents or by siRNA stimulated OC cell death and

increased chemosensitivity (Bao et al., 2015; Sun et al., 2015; Tan et al., 2019).

Recently, the emerging tumour suppressor effect of glucagon-like peptide 1 (GLP-1) has attracted attention of scientists. GLP-1 was initially identified as an insulinotropic intestinal hormone, but its short half-life limited its clinical application (Holst, 2007). Exendin-4 (exenatide), a 39-amino acid peptide amide, is a long-acting GLP-1 receptor agonist that is currently used to improve glycaemic control in type 2 diabetes patients (Yap and Misuan, 2019). The tumour-suppressive effect of exendin-4 has been demonstrated in a variety of solid tumours and different mechanisms for its action have been identified. Exendin-4 inhibited progression of prostate cancer and breast cancer through inhibition of ERK-MAPK, NF- κ B, and Bcl-2 (Nomiya et al., 2014; Tsutsumi et al., 2015; Zhang et al., 2016; Iwaya et al., 2017). Also, exendin-4 inhibited endometrial cancer proliferation and induced apoptosis by activation of AMPK-induced inhibition of mTOR (Zhang et al., 2016). He et al. have shown that exendin-4 can suppress the growth, migration, and invasion of OC cells and stimulate apoptosis through inhibition of the PI3K/Akt pathway (He et al., 2016). Recently, our group has shown that the anti-tumour effects of exendin-4 in two OC cell lines involved activation of silent inflammatory regulator 1 (SIRT 1) and inhibition of NF- κ B (Khaleel et al., 2020).

By integrating the knowledge of the signalling pathways influenced by exendin-4 (PI3K/Akt, AMPK) and given the relation of these two pathways to mTOR and autophagy, it is possible to suggest that the tumour suppressor effect of exendin-4 in OC involves modulation of autophagy. In support of this view, exendin-4 stimulated autophagy in the brains of diabetic rats as well as in palmitate-treated β -cells (Zummo et al., 2017; Candéas et al., 2018). Also, exendin-4 prevented hepatic steatosis in mice and improved their survival by promoting autophagy (Sharma et al., 2011). Interestingly, exendin-4 inhibited cell proliferation and growth in a liver hepatocellular carcinoma cell line (HepG2) through the activation of autophagy (Krause et al., 2019).

Hence, in this study, we hypothesize that the anti-tumour effects of exendin-4 in SKOV-3 and OVCAR-3 OC cell lines involve activation of autophagy. Also, we investigated the involvement of PI3K/Akt/mTOR and AMPK signalling pathways in the exendin-4 anti-tumour effect.

Material and Methods

Cell lines

Two ovarian cancer cell lines, SKOV-3 and OVCAR-3, were purchased from American Type Culture Collection (Manassas, VA). Both cell lines were grown in Dulbecco's modified Eagle's medium (DMEM) (without phenol red), under humidified atmosphere (95% air, 5% CO₂, 37 °C). The medium was supplemented with

100 µg/ml of streptomycin, 100 units/ml of penicillin, 10% foetal bovine serum (FBS), and 2 mM glutamine (ThermoFisher Scientific Inc, Waltham, IL) according to the supplier's recommendation.

Experimental procedure

Cells were initially cultured at a density of 1×10^5 /ml for 24 h to reach 85% confluence, and then were used in the experimental procedure. OC cells were incubated for 24 h in the presence or absence of exendin-4 (30 µM for SKOV-3 and 40 µM for OVCAR-3) (Cat. No. E7144, > 97%, Sigma Aldrich, St. Louis, MO) with or without pre-incubation with 10 µM chloroquine (CQ), an autophagy inhibitor (Cat. No. C6628). Cells were also incubated with exendin-4 at the doses mentioned above for 24 h with or without one-hour pre-incubation with 10 µM compound C (CC), an AMPK inhibitor, or 10 µM insulin-like growth factor-1 (IGF-1), a PI3K/Akt activator. The concentrations of exendin-4 for both cell lines used in this study were pre-determined in previous studies on both SKOV-3 and OVCAR-3 OC cell lines, where these concentrations represented the effective half inhibitory concentration (IC_{50}) to inhibit cell survival and growth under similar conditions (Khaleel et al., 2020). Exendin-4 and IGF-1 were always dissolved in the media, whereas CQ and CC were freshly prepared in DMSO (Cat. No. 472301, Sigma Aldrich). Control cells were treated with DMSO. The final concentration of DMSO in the media was always less than 0.1 %. DMSO at this concentration was tested in preliminary studies and did not affect any of the measured parameters. All experiments were performed in three independent experiments, each performed in triplicate.

Determination of cell viability

Cell viability was determined in all experimental groups using the cell counting kit-8 (CCK-8) (Cat No. CK04-13, Dojindo Molecular Technologies, Taipei City, Japan). In brief, 100 µl of the culture medium was discarded at the end of the incubation period, replaced with new fresh medium containing 10 % of CCK8 solution, and incubated for an extra three h at 37 °C. After incubation, the absorbance of all samples was measured at 450 nm using a Spectramax plate reader (model M2, Molecular Devices, San Jose, CA). Cell viability was calculated as a percent of the control (SKOV-3 untreated). The assay followed the manufacturer's instructions.

Measurements of levels of LDH activity

To evaluate cytotoxicity and plasma membrane damage, LDH activity was determined in cell supernatants using a commercially available kit (Cat. No. ab102526; Abcam, Cambridge, UK) according to the manufacturer's instructions. The test relies on measuring the absorbance of the colour produced by the interaction of the produced NADPH with a specific probe. In the test, NADPH is produced by the reduction of NAD^+ in the presence of LDH in the sample. In brief, samples were centrifuged ($200 \times g$, 5 min, 4 °C) and their supernatants

were collected. Then, 20 µl of the sample or standard was incubated with 2 µl of the LDH substrate mix and 48 µl of LDH assay buffer. The developed colour was read at 450 nm every 3 min for 30 min in a Spectramax plate reader (Model M2, Molecular Devices). The activity of LDH (nmol/min/ml) = (mU/ml) (U/l) was calculated from an NADH standard curve (nmol) and using the equation = $(B/\Delta T \times V) \times DF$, where B = the amount of NADH in the sample well calculated from the standard curve (nmol), ΔT = reaction time (min). V = original sample volume added into the reaction well (ml), and d = sample dilution factor. One unit of LDH = the amount of enzyme that catalyses the conversion of lactate to pyruvate to generate 1.0 µmol of NADH per minute at pH 8.8 at 37 °C.

Measurement of cell proliferation

Cell proliferation was determined by a bromo-2'-deoxyuridine (BrdU) ELISA kit (Cat. No. 11647229001; Roche Diagnostics, Indianapolis, IN). The principle of the test relies on the incorporation of BrdU into newly synthesized cellular DNA, which can then be detected by using specific BrdU-peroxidase (POD) and a substrate reagent, 3,3',5,5'-tetramethylbenzidine. Briefly, the cells were cultured with various treatments in a final volume of 100 µl for 24 h. Then, 10 µl of BrdU was added to each well and incubated for 2 h at 37 °C. Then, the medium was removed, and 200 µl FixDena (a denaturation reagent provided with the kit) was added to each well and incubated for 30 min at 23 °C. The FixDena solution was removed, and 100 µl POD solution was added to each well and incubated at 23 °C for 90 min. The solution was then removed and each well was washed three times with 200 µl of the washing solution (PBS). Then, 10 µl of the substrate reagent was added to each well and incubated at 23 °C for 15 min until the colour developed. Absorbance was read at 370 nm (reference range 492 nm) in a Spectramax plate reader (model M2, Molecular Devices). Cell proliferation was calculated as a percent of the control.

Quantitative measurement of apoptosis by ELISA

Cell apoptosis in all treatments was quantified by a cell death detection ELISA plus kit (Cat. No. 11 920 685 001, Roche Diagnostics GmbH, Mannheim, Germany). The kit measures both mono- and oligonucleosomes by a unique anti-histone antibody that can react with H1, H2A, H2B, H3, and H4 and a peroxidase-conjugated DNA antibody that can bind to single- and double-stranded DNA. In brief, cells were centrifuged at $200 \times g$ for 10 min and the supernatant was removed. Then, 200 µl of the lysis buffer was added to each well, incubated for 30 min at room temperature, and then centrifuged at $200 \times g$ for 10 min. After that, 20 µl of the supernatant was transferred into the provided streptavidin-coated microplate followed by addition of 80 µl of the prepared

immunoreagent to each well. The plate was covered with adhesive foil and incubated at room temperature under gentle shaking for two hours. The solution was removed, and wells were washed three times with 200 μ l of the incubation buffer. Then, the solution was removed and 100 μ l of ABTS solution was added to each well and incubated under shaking for an additional 20 min at room temperature until the colour developed. The absorbance was read at 405 nm (reference range 490) against ABTS solution as a blank using a Spectramax plate reader (model M2, Molecular Devices).

Cell migration and invasion

To assess the rate of cell migration, cells were cultured in serum-free medium at a density of 1×10^5 /ml (100 μ l) at the top of 8- μ m pore Corning 24-well Transwell polycarbonate inserts (Corning Incorporated, Corning, NY) and treated as described by the manufacturer. The lower chamber was filled with 600 μ l of DMEM containing 10% FBS as an attractant. After 24 h, migrating cells at the bottom of the filter were fixed with methanol (15 min, room temperature) and then stained with crystal violet (0.2%) for 15 min. Cells were counted under a light microscope (10 \times) in five random fields. The same procedure was applied in the invasion assay, but with the use of 5- μ m Transwell polycarbonate chamber plates pre-coated with 50 μ l Matrigel (Cat. No. DLW354263, Sigma Aldrich). In this test, the cells were first fasted for three hours in serum-free media and then loaded into the chamber.

Measurements of GSH

Levels of glutathione (GSH) in the cell lysates were measured using a commercially available kit (Cat. No. 7511-100-K, Trevigen, Gaithersburg, MD). The kit is based on the optimized enzymatic recycling method for quantification of GSH, which utilizes glutathione reductase (GRx) that reduces the oxidized glutathione (GSSG) to reduced glutathione (GSH). Then, the sulfhydryl group of GSH reacts with 5,5'-dithiobis-2-nitrobenzoic acid (DTNB) to produce yellow-coloured 5-thio-2-nitrobenzoic acid (TNB) that can be read at 405 nm and indicates the levels of GSH in the sample. In the test, the levels of total GSH and GSSG were calculated from the GSSG standard curve and the levels of reduced GSH were calculated using the formula reduced GSH = total GSH-GSSG. Preparation of the cell lysates and reagents, as well as the assay protocol, were carried out as described by the kit and in accordance with the manufacturer's instructions.

Preparation of the nuclear extract and cell homogenates for Western blotting

Nuclear proteins were separated from the frozen cells of all treatments by using a commercially available kit (NE-PER) (Cat. NO. 78833, Thermo Fisher Scientific, Waltham, MA). To prepare total cell homogenates, the

cells were pelleted and homogenized (1×10^5 /ml) in 200 μ l of RIPA buffer (Cat. No. a56034, Abcam, Cambridge, UK) plus 5 μ l protease inhibitor (Cat. No. P8340 Sigma-Aldrich). The supernatants of these homogenates were collected after centrifugation ($11,000 \times g/4^\circ\text{C}/10$ min). The protein levels in the nuclear extract and total cell homogenates were determined using a Pierce BCA Protein Assay Kit (Cat. No. 23225, Thermo Fisher Scientific). Antibodies used in the Western blotting protocol, see Table 1 (Cell Signalling Technology, Danvers, MA).

Western blot analysis

Samples were prepared in the loading buffer, boiled, then loaded (40 μ g/well), and separated using 8–12% SDS-polyacrylamide gel. Proteins were then transferred onto nitrocellulose membranes (Cat. No. sc-3718, Santa Cruz Biotechnology, Dallas, TX). Membranes were blocked for 2 h with 5% (w/v) non-skimmed milk (prepared in TBST buffer). After successful washing (3 \times , 10 min, TBST), the membranes were incubated with continuous shaking with the primary antibodies for 2 h at room temperature. Then, the membranes were washed again and incubated with the corresponding horseradish peroxidase (HRP)-conjugated secondary antibody for another 2 h at room temperature. Chemiluminescence was detected using a Pierce ECL kit (Thermo Fisher Scientific). All images were scanned and analysed using a C-Di Git blot scanner (LI-COR, Lincoln, NE). All antibodies were diluted in the TBST buffer. The washing between steps was done in triplicate (each of 10 min) using the TBST buffer. Membranes were stripped up to five times, and phosphorylated forms were detected first. A known control sample was run between gels to standardize the readings. The relative expression of total proteins was normalized by the expression of the reference cytoplasmic protein, β -actin, whereas the relative expression of the nuclear proteins (NF- κ B) was normalized to the nuclear reference protein, lamin B1.

Statistical analysis

Statistical analysis was performed using the GraphPad Prism statistical software package (version 6). Differences among control and exendin-4-treated cells were determined by the Student's *t*-test. The differences among all the other groups were assessed by one-way ANOVA, followed by Duncan's multiple range test. Data were presented as mean \pm SD. Values were considered significantly different when $P < 0.05$.

Results

Exendin-4 enhanced autophagy markers in both SKOV-3 and OVCAR-3 cell lines

Activation of beclin-1 and conversion of LC3I to LC3II, as well as the decrease in protein expression of p62, are considered major markers for activation of au-

Table 1. Antibodies used in the Western blotting protocol

Target	Cat. No.	Manufacturer	KDa	Dilution
Akt	9272	Cell Signalling Technology	60	1 : 1000
p-Akt (Thr ³⁰⁸)	9275	Cell Signalling Technology	60	1 : 1000
AMPK- α 1	2532	Cell Signalling Technology	62	1 : 250
p-AMPK- α 1 (Thr ¹⁷²)	2535	Cell Signalling Technology	62	1 : 250
p-raptor (Ser ⁷⁹²)	2083	Cell Signalling Technology	150	1 : 500
p-S6K1 (Thr ³⁸⁹)	9205	Cell Signalling Technology	70/85	1 : 500
p- 4E-BP1 (Thr ^{37/46})	2855	Cell Signalling Technology	18	1 : 250
Bcl-2	2876	Cell Signalling Technology	28	1 : 1000
Bax	2772	Cell Signalling Technology	20	1 : 1000
Cleaved caspase-3	9664	Cell Signalling Technology	17/19	1 : 1000
Cleaved caspase-8	9496,	Cell Signalling Technology	18	1 : 500
Beclin-1	3738	Cell Signalling Technology	60	1 : 1000
p62	5114	Cell Signalling Technology	62	1 : 1000
p-NF- κ B p65	3030	Cell Signalling Technology	65	1 : 500
LC3I/II	2727	Cell Signalling Technology	14/16	1 : 1000
β -Actin	3700	Cell Signalling Technology	45	1 : 2000
Lamin B	12586	Cell Signalling Technology	60	1 : 2000

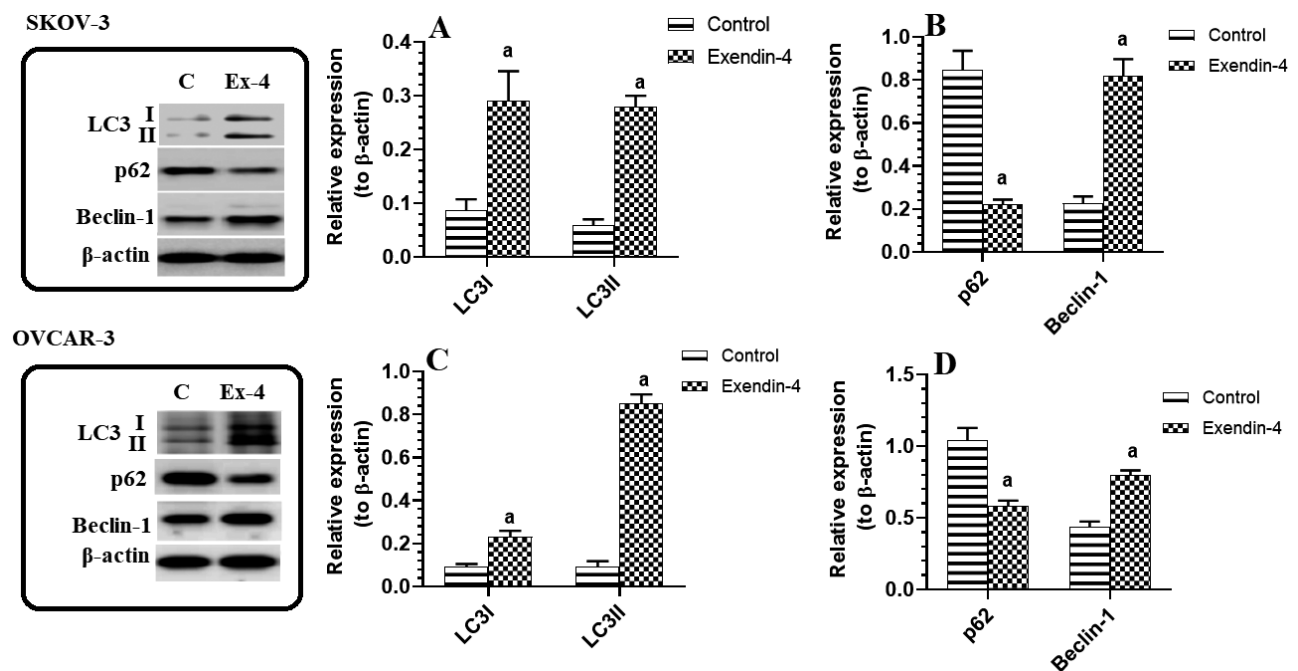


Fig. 1. Exendin-4 activates LC3-I/II and beclin-1, major autophagy markers, and inhibits p62, a major target of autophagy in both treated SKOV-3 and OVCAR-3 cells. Cells were cultured at a density of 1×10^5 /ml in DMEM medium for 24 h and treated with exendin-4 (30 μ M for SKOV-3 and 40 μ M for OVCAR-3). Control cells were treated with 0.1% DMSO. Data are presented as mean \pm SD. ^a Significantly different as compared to control cells.

tophagy. To test the effect of exendin-4 on the process of autophagy, we initially measured the protein expression of all these markers in the control and exendin-4-treated cells. Treatment of the SKOV-3 cells with exendin-4 at the tested IC₅₀ (30 μ M) significantly up-regulated the

protein levels of LC3I (0.08 ± 0.001 vs 0.29 ± 0.045) (262.6 ± 46 %), LC3II (0.06 ± 0.008 vs 0.28 ± 0.016) (362 ± 32 %), and beclin-1 (0.26 ± 0.02 vs 0.81 ± 0.12) (209 ± 38 %), but significantly decreased the protein levels of p62 (0.82 ± 1.3 vs 0.22 ± 0.04) (70.4 ± 8.4 %)

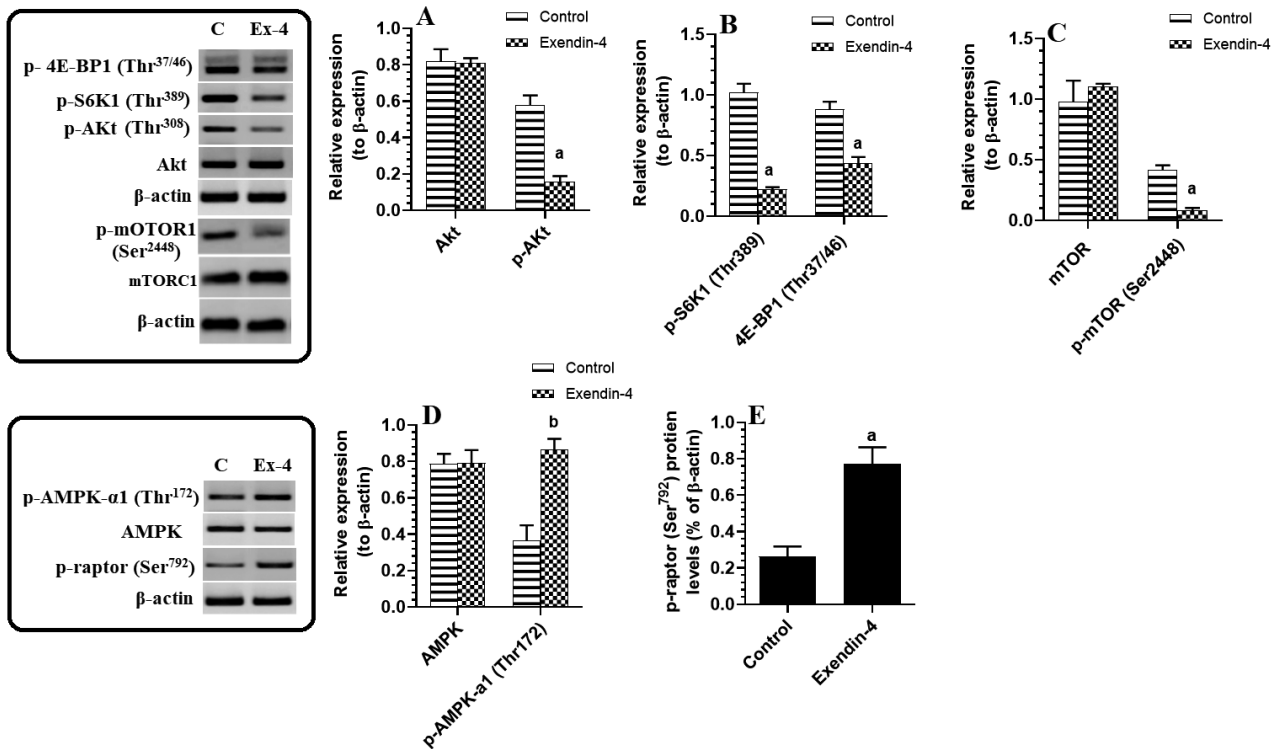


Fig. 2. Exendin-4 suppresses Akt and mTOR signalling and activates AMPK in the treated SKOV-3 cells. Cells were cultured at a density of 1×10^5 /ml in DMEM medium for 24 h and treated with exendin-4 (30 μ M for SKOV-3). Control cells were treated with 0.1% DMSO. Data are presented as mean \pm SD. ^a Significantly different as compared to control cells. ^b Significantly different as compared to exendin-4-treated cells.

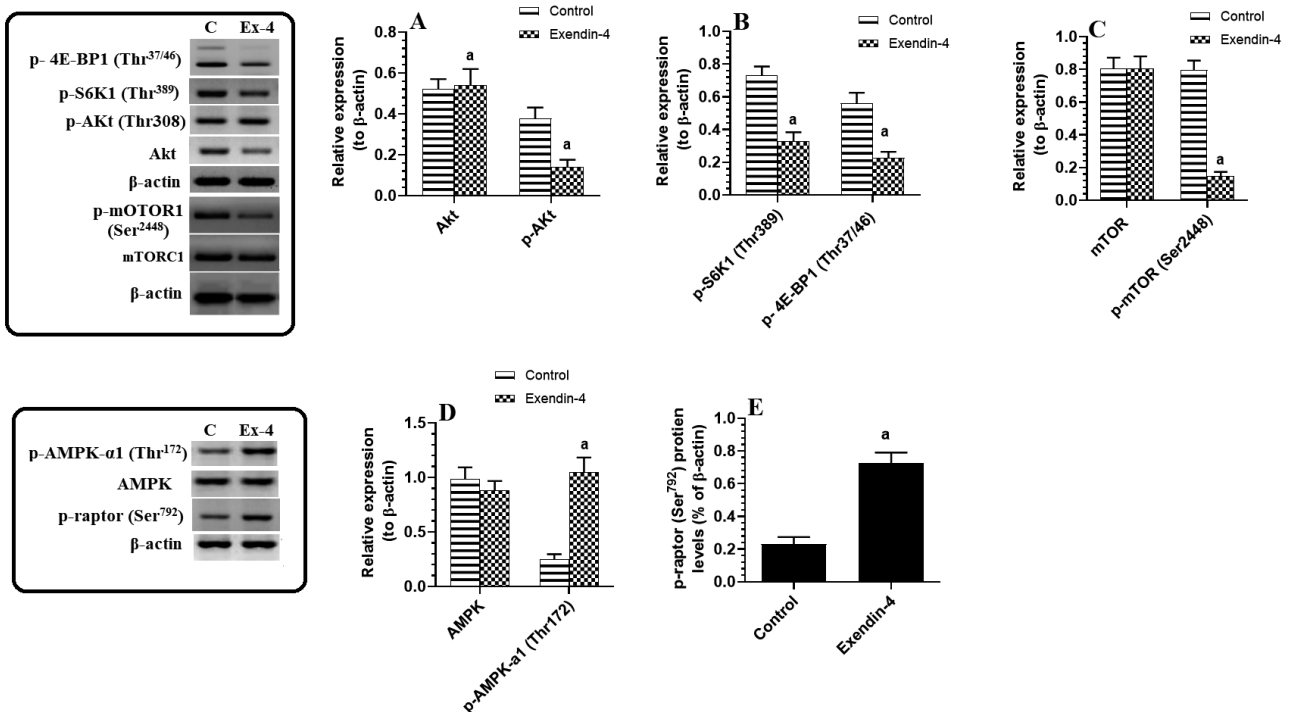


Fig. 3. Exendin-4 suppresses Akt and mTOR signalling and activates AMPK in the treated OVCAR-3 cells. Cells were cultured at a density of 1×10^5 /ml in DMEM medium for 24 h and treated with exendin-4 (40 μ M for OVCAR-3). Control cells were treated with 0.1% DMSO. Data are presented as mean \pm SD. ^a Significantly different as compared to control cells.

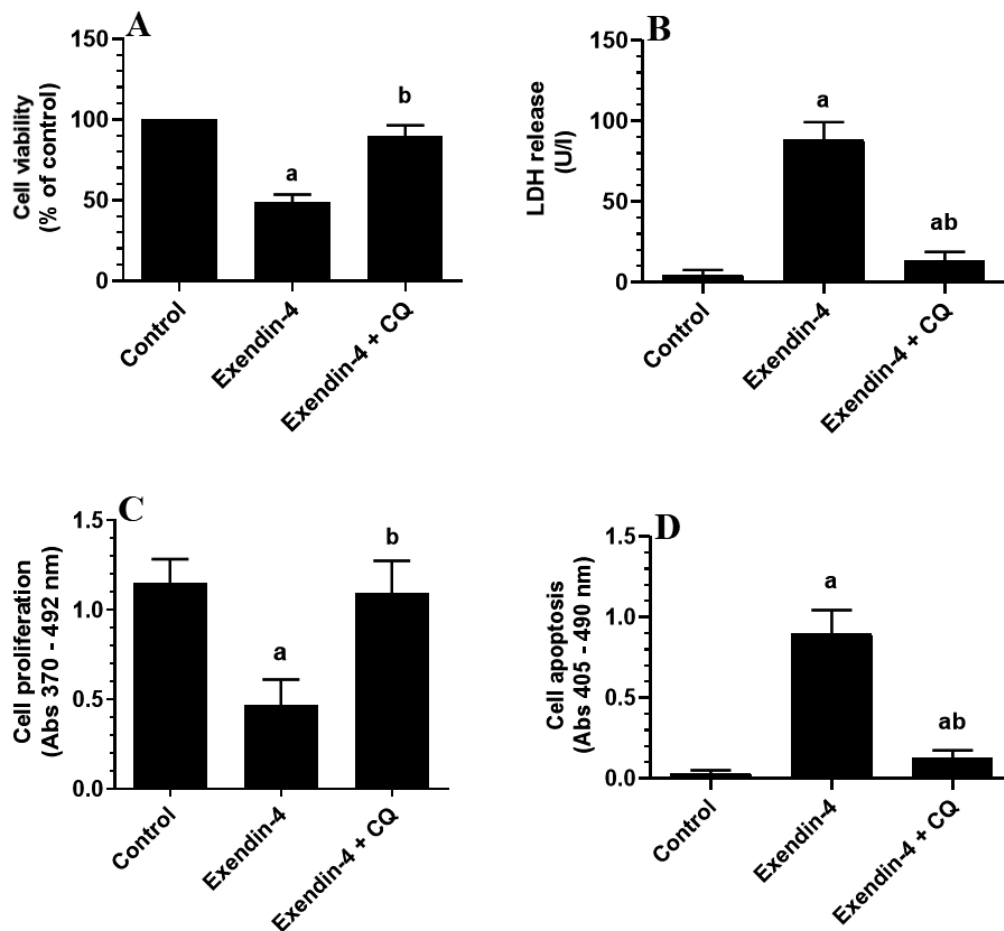


Fig. 4. Chloroquine (CQ), an autophagy inhibitor, prevents exendin-4-induced suppression of cell survival and proliferation and stimulation of cell apoptosis and LDH release in the treated SKOV-3 cells. Cells were cultured at a density of 1×10^5 /ml in DMEM medium for 24 h and treated with exendin-4 (30 μ M for SKOV-3). Control cells were treated with 0.1% DMSO. Data are presented as mean \pm SD. ^a Significantly different as compared to control cells. ^b Significantly different as compared to exendin-4-treated cells.

as compared to control untreated cells (Fig. 1 A,B). In the same way, and as compared to control cells, treatment of the OVCAR-3 cells with exendin-4 at an IC_{50} of 40 μ M significantly increased the levels of LC3I (0.09 ± 0.009 vs 0.23 ± 0.02) (155 ± 15.6 %), LC3II (0.093 ± 0.02 vs 0.85 ± 0.13) (743 ± 87 %), and beclin-1 (0.43 ± 0.53 vs 0.80 ± 0.22) (85.6 ± 7.4 %) and concomitantly decreased the protein levels of p62 (1.0 ± 0.15 vs 0.58 ± 0.08) (47.3 ± 4.8 %) as compared to untreated cells (Fig. 1C,D). These data indicated that exendin-4 activates autophagy markers in both SKOV-3 and OVCAR-3 cells.

Exendin-4 inhibits mTORC1 and Akt but activates AMPK in both SKOV-3 and OVCAR-3 cell lines

mTORC1 is a potent inhibitor of autophagy. Akt activates but AMPK inhibits mTORC1. However, p-4E-BP1 and S6K1 are the major downstream targets of mTORC1, whereas raptor is the most common downstream target

of AMPK. The total levels of mTOR, Akt, and AMPK remained significantly unchanged between the control and exendin-4-treated SKOV-3 or OVCAR-3 cells (Figs. 2 and 3). However, exendin-4 significantly reduced the protein levels of p-mTOR (Ser²⁴⁴⁸) (89.4 ± 4.8 % and 81.3 ± 6.7 %), p-4E-BP1 (Thr^{37/46}) (50.2 ± 5.3 % and 59.3 ± 6.7 %), and p-S6K1 (Thr³⁸⁹) (78.9 ± 4.3 % and 54.7 ± 8.2 %) in both the treated SKOV-3 and OVCAR-3 cells, respectively and as compared to their control cells (Fig. 2A–C and Fig. 3A–C). Concomitantly, exendin-4 significantly decreased the protein levels of p-Akt (73.5 ± 7.8 % & 63.2 ± 10 %) but increased the protein levels of p-AMPK (Thr¹⁷²) (142.5 ± 15 % and 337.5 ± 34.3 %) and p-raptor (Ser⁷⁹²) (271 ± 43 % and 277.8 ± 35 %) in both the treated SKOV-3 and OVCAR-3 cells, respectively, as compared to their control untreated cells (Fig. 2D,E and Fig. 3D,E). These data confirm that the exendin-4-induced activation of autophagy markers in both OC cell lines is accompanied by inhibition of mTORC1 and Akt and activation of AMPK.

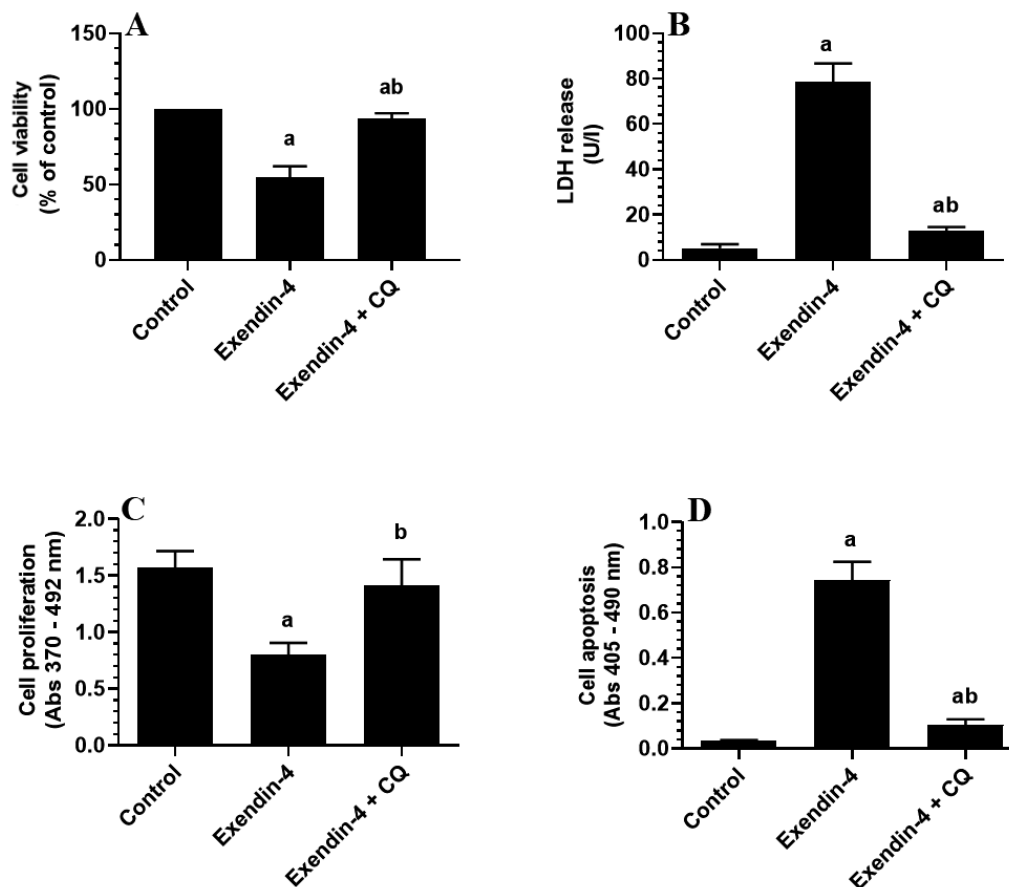


Fig. 5. Chloroquine (CQ), an autophagy inhibitor, prevents exendin-4-induced suppression of cell survival and proliferation and stimulation of cell apoptosis and LDH release in the treated OVCAR-3 cells. Cells were cultured at a density of 1×10^5 /ml in DMEM medium for 24 h and treated with exendin-4 (40 μ M for OVCAR-3). Control cells were treated with 0.1% DMSO. Data are presented as mean \pm SD. ^a Significantly different as compared to control cells. ^b Significantly different as compared to exendin-4-treated cells.

Exendin-4-induced autophagy markers indicate a cytotoxic, apoptotic, and tumour invasiveness suppressive effect

Chloroquine (CQ) is the most accepted autophagy inhibitor approved by the FDA (Manic et al., 2014). To determine whether exendin-4-induced activation of autophagy markers is a protective or cytotoxic signal, we measured cell survival and apoptosis and determined the levels of LDH in the media and cell migration and invasion in exendin-4-treated OC cell lines in the presence or absence of CQ (Figs. 4–6). Exendin-4 significantly reduced cell survival (46 ± 5.6 % and 52.7 ± 8.3 %) and the absorbance of cell proliferation (50.3 ± 7.6 % and 55.5 ± 10.2 %), but significantly increased the absorbance of cell apoptosis (1440 ± 221 % and 1560 ± 179 %), as well as the medium levels of LDH (873 ± 163 % and 1500 ± 298 %) in both SKOV-3 and OVCAR-3 cells, respectively, as compared to control untreated cells (Fig. 4A,D and Fig. 5A,D). Besides, exendin-4 significantly reduced cell invasion ($45.5 \pm$

5.5 % and 51.3 ± 6.2 %) and migration (43.7 ± 6.2 % and 52.8 ± 7.3 %) in both the SKOV-3 and OVCAR-3 cells, respectively, and as compared to control untreated cells (Fig. 6A–D). On the other hand, pre-treatment with exendin-4 with CQ completely reversed all these events both in the treated SKOV-3 and OVCAR-3 cells. While the cell survival, absorbance of cell proliferation, migration, and invasion of both the SKOV-3 and OVCAR-3 cells treated in the presence of CQ led to return to their basal levels, the absorbance of cell apoptosis and the levels of LDH in both groups of treated cells remained slightly but significantly higher than their basal levels observed in control untreated cells (Fig. 4A–D, Fig. 5A–D and Fig. 6A–D).

Exendin-4 induces cell apoptosis, inhibits NF- κ B p65 and suppresses GSH levels in an autophagy-dependent manner

Autophagy can induce apoptosis and suppress inflammation and antioxidant levels by down-regulating p62

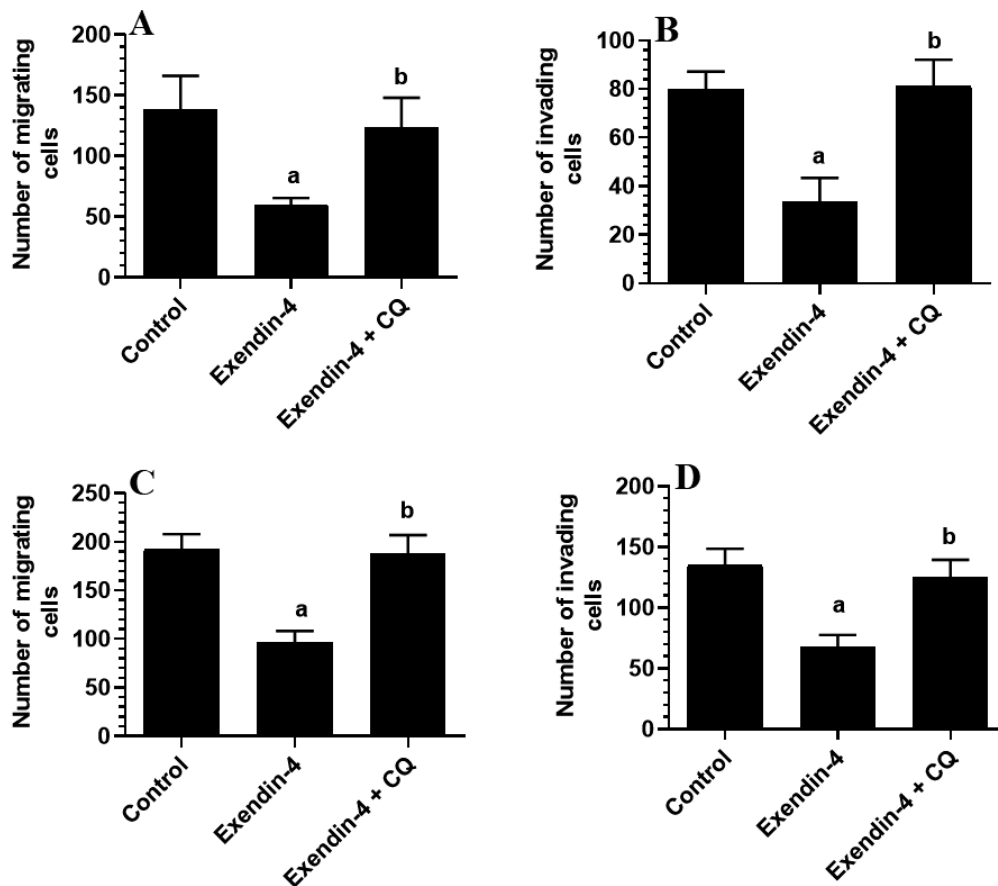


Fig. 6. Chloroquine (CQ), an autophagy inhibitor, inhibits exendin-4-induced reduction in migrating and invading cells in the treated SKOV-3 and OVCAR-3 cells. Cells were cultured at a density of 1×10^5 /ml in DMEM medium for 24 h and treated with exendin-4 (30 μ M for SKOV-3 and 40 μ M for OVCAR-3). Control cells were treated with 0.1% DMSO. Data are presented as mean \pm SD. ^a Significantly different as compared to control cells. ^b Significantly different as compared to exendin-4-treated cells.

arm. In both SKOV-3 and OVCAR-3 cells, exendin-4 significantly reduced the levels of glutathione (GSH) (27.8 ± 4.4 vs 10.2 ± 2.6 (61.2 \pm 7.5 %) for SKOV-3 and 34.5 ± 5.1 vs 12.8 ± 3.2 (62.4 \pm 10.2) for OVCAR-3), lowered the protein expression of Bcl-2 (0.92 ± 0.17 vs 0.43 ± 0.07) (49.3 \pm 6.4 %) for SKOV-3 and (0.45 ± 0.09 vs 0.21 ± 0.02) (54.4 \pm 7.2 %) for OVCAR-3), and increased the protein levels of Bax (0.29 ± 0.6 vs 0.93 ± 0.13) (365 \pm 32 %) for SKOV-3 and (0.06 ± 0.01 vs 0.173 ± 0.32) (206 \pm 28.4 %) for OVCAR-3), as compared to control untreated cells (Fig. 7A,C). Also, exendin-4 significantly reduced the level of nuclear p-NF- κ B p65 (Ser⁵³⁶) in both SKOV-3 and OVCAR-3 cells ((0.82 ± 0.23 vs. 0.11 ± 0.03) (85.4 \pm 6.2 %) and (0.63 ± 0.13 vs. 0.05 ± 0.02) (79.3 \pm 7.8 %), respectively) (Fig. 8A,B). Exendin-4 also increased the protein levels of caspase-3 (0.04 ± 0.01 vs 0.47 ± 0.06) (1397 \pm 121 %) and (0.08 ± 0.01 vs 0.43 ± 0.42) and protein levels of caspase-8 (0.1 ± 0.02 vs 0.63 vs. 0.04) (535.4 \pm 63 %) (0.07 ± 0.02 vs 0.42 ± 0.56) (473 \pm 33 %) in both the SKOV-3 and OVCAR-3 cells, respectively (Fig. 8C,D).

Interestingly, normal levels of GSH and protein expression of Bcl-2, cleaved caspase-3 and cleaved caspase-8, which are not significantly different with their corresponding levels in the control cells, were observed in both SKOV-3 and OVCAR-3 cells that were pre-treated with exendin-4 + CQ (Fig. 7A–D and Fig. 8A–D).

AMPK activation and Akt suppression are required for exendin-4-induced activation of autophagy markers in both SKOV-3 and OVCAR-3 cells

To further confirm that mTORC1 inhibition was mediated by concomitant activation of AMPK and inhibition of Akt signalling pathways, we treated both cell lines with exendin-4 with or without pre-incubation with CC, an AMPK inhibitor, and IGF-1, a PI3K/Akt/mTORC1 activator. As expected, individual treatment with CC or IGF-1 increased cell survival (41.2 ± 4.3 % and 42.9 ± 5.2 %, respectively) and reduced the absorbance of cell apoptosis (52 ± 8.3 % and 54.5 ± 10.3 %, respectively).

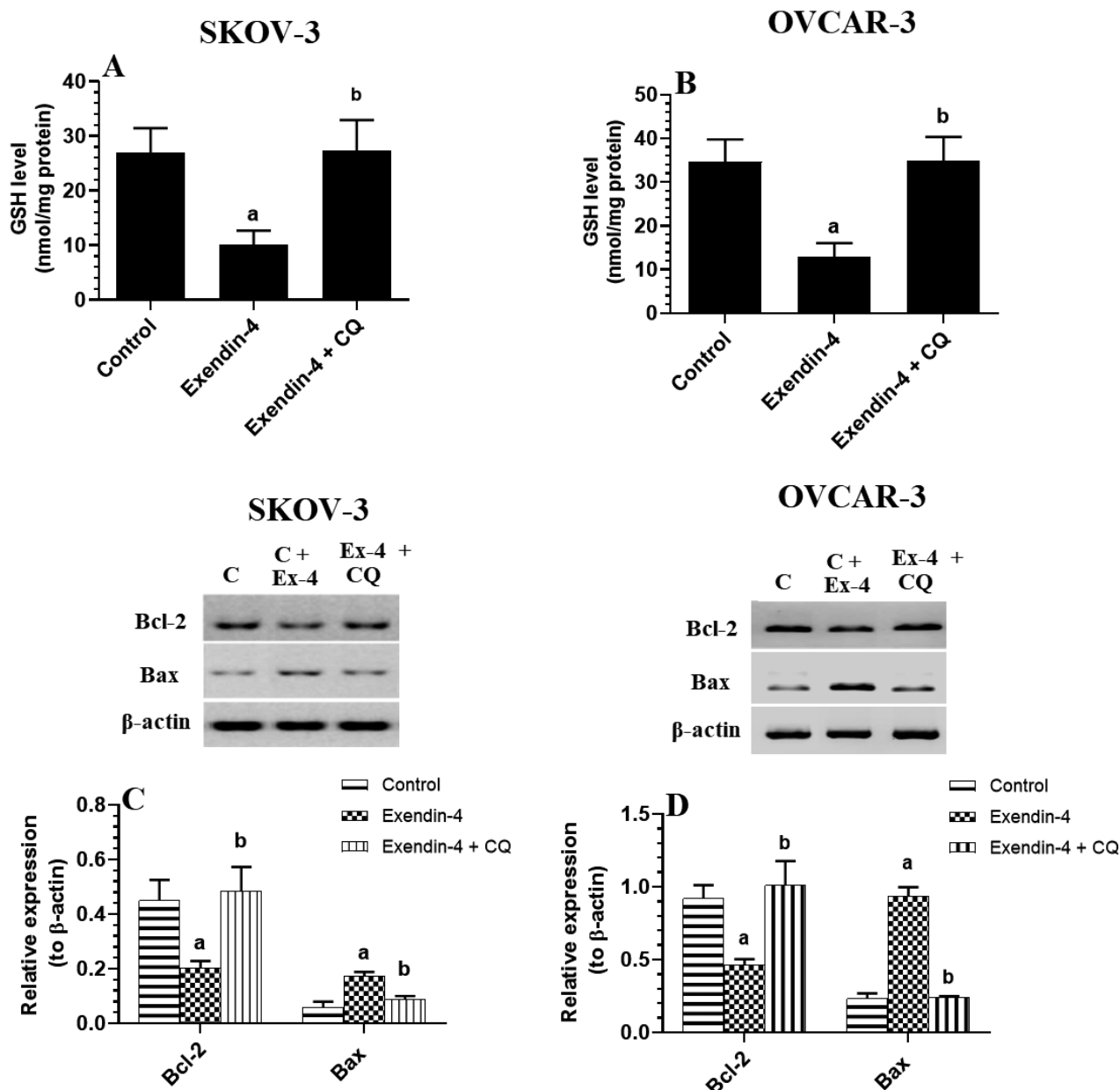


Fig. 7. Chloroquine (CQ), an autophagy inhibitor, inhibits exendin-4 induced reduction in GSH levels and expression of Bcl-2 and up-regulation of Bax in the treated SKOV-3 and OVCAR-3 cells. Cells were cultured at a density of 1×10^5 /ml in DMEM medium for 24 h and treated with exendin-4 (30 μ M for SKOV-3 and 40 μ M for OVCAR-3). Control cells were treated with 0.1% DMSO. Data are presented as mean \pm SD. ^a Significantly different as compared to control cells. ^b Significantly different as compared to exendin-4-treated cells.

respectively) and LDH release ($27.3 \pm 4.7\%$ and $32.6 \pm 3.7\%$, respectively) in the treated SKOV-3 cells as compared to exendin-4-treated cells (Fig. 9A–C). Also, exendin-4 + CC and exendin-4 + IGF-1-treated SKOV-3 cells showed a significant increase in the expression of p62 ($71.8 \pm 3.4\%$ and $72.7 \pm 4.8\%$, respectively) with a concomitant decrease in the protein levels of beclin-1 ($60.4 \pm 6.5\%$ and $66.8 \pm 7.3\%$, respectively), LC3I ($50.4 \pm 3.6\%$ and $51.6 \pm 5.8\%$, respectively, and LC3II ($57.4 \pm 6.2\%$ and $16.3 \pm 2.8\%$) as compared to exendin-4-treated cells (Fig. 9D,E).

Likewise, a partial increase in cell survival ($44.3 \pm 4.5\%$ and $48.7 \pm 5.1\%$) with a parallel partial decrease in the absorbance of cell apoptosis ($71.4 \pm 6.2\%$ and $74.1 \pm 5.8\%$) and LDH levels ($49.5 \pm 3.4\%$ and $61.3 \pm 5.3\%$) were observed in exendin-4 + IGF and exendin-4 + CC-treated OVCAR-3 cells, respectively, and as compared to exendin-4-treated cells (Fig. 10A–C). Concomitantly, a significant increase in the protein level of p62 (5.5 and 2 fold, respectively), with a concomitant reduction in LC3I ($37.8 \pm 3.1\%$ and $81.4 \pm 5.2\%$), LC3II ($87.5 \pm 7.1\%$ and $91.3 \pm 6.3\%$), and beclin-1

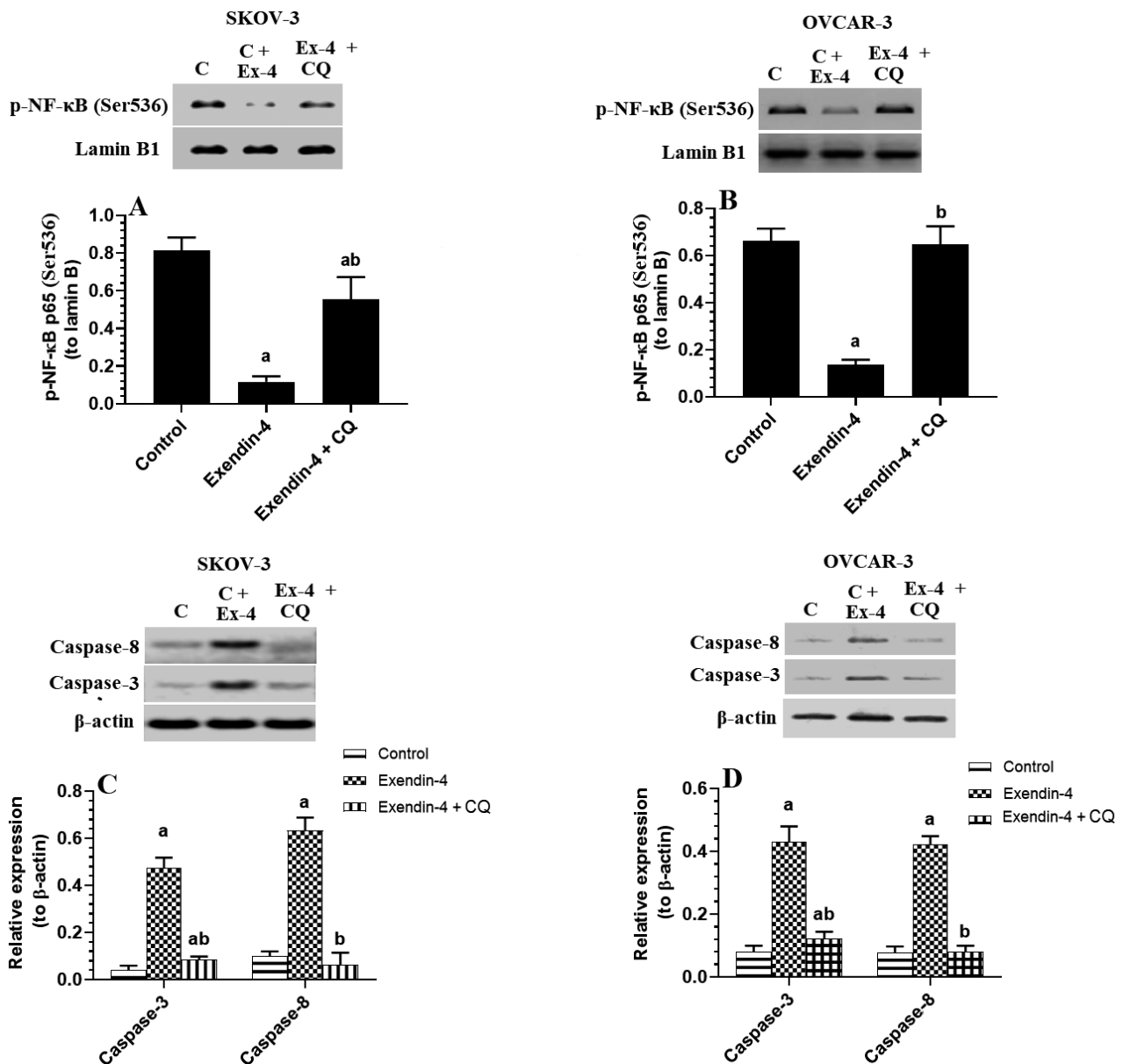


Fig. 8. Chloroquine (CQ), an autophagy inhibitor, suppresses exendin-4-induced inhibition of the nuclear activation of NF-κB and up-regulation of caspases 3 and 8 in the treated SKOV-3 and OVCAR-3. Cells were cultured at a density of 1×10^5 /ml in DMEM medium for 24 h and treated with exendin-4 (30 μ M for SKOV-3 and 40 μ M for OVCAR-3). Control cells were treated with 0.1% DMSO. Data are presented as mean \pm SD. ^a Significantly different as compared to control cells. ^b Significantly different as compared to exendin-4-treated cells.

(48.9 ± 5.9 % and 58.9 ± 6.9 %) were observed in exendin-4 + IGF-1 and exendin-4 + CC-treated cells and as compared to exendin-4-treated cells (Fig. 10D,F). However, the levels of all these parameters in both treated SKOV-3 and OVCAR-3 cells remained significantly different from their corresponding levels observed in the control group, thus suggesting partial effects. However, SKOV-3 and OVCAR-3 cells that were treated with the combination of CC and IGF-1 exhibited the maximum increase in cell survival (82.4 ± 6.7 % for SKOV-3 and 87.3 ± 5.9 % for OVCAR-3) and maximum decrease in cell apoptosis absorbance (80.5 ± 5.9 % for SKOV-3

and 82.4 ± 8.7 % for OVCAR-3) and LDH release (84 ± 7.3 % for SKOV-3 and 78.8 ± 9.4 % for OVCAR-3) as compared to exendin-4-treated cells (Fig. 9A–C and Fig. 10A–C). In addition, treatment of SKOV-3 and OVCAR-3 cells with the combined CC and IGF-1 restored normal levels of p62, beclin-1, and LC3I, which were not significantly different as compared to their levels depicted in the control untreated cells (Fig. 9D–E and Fig. 10D–E). Overall, these data indicate that concurrent activation of AMPK and inhibition of Akt are crucial for exendin-4 suppression of cell death, induction of apoptosis, and activation of cytotoxic autophagy markers.

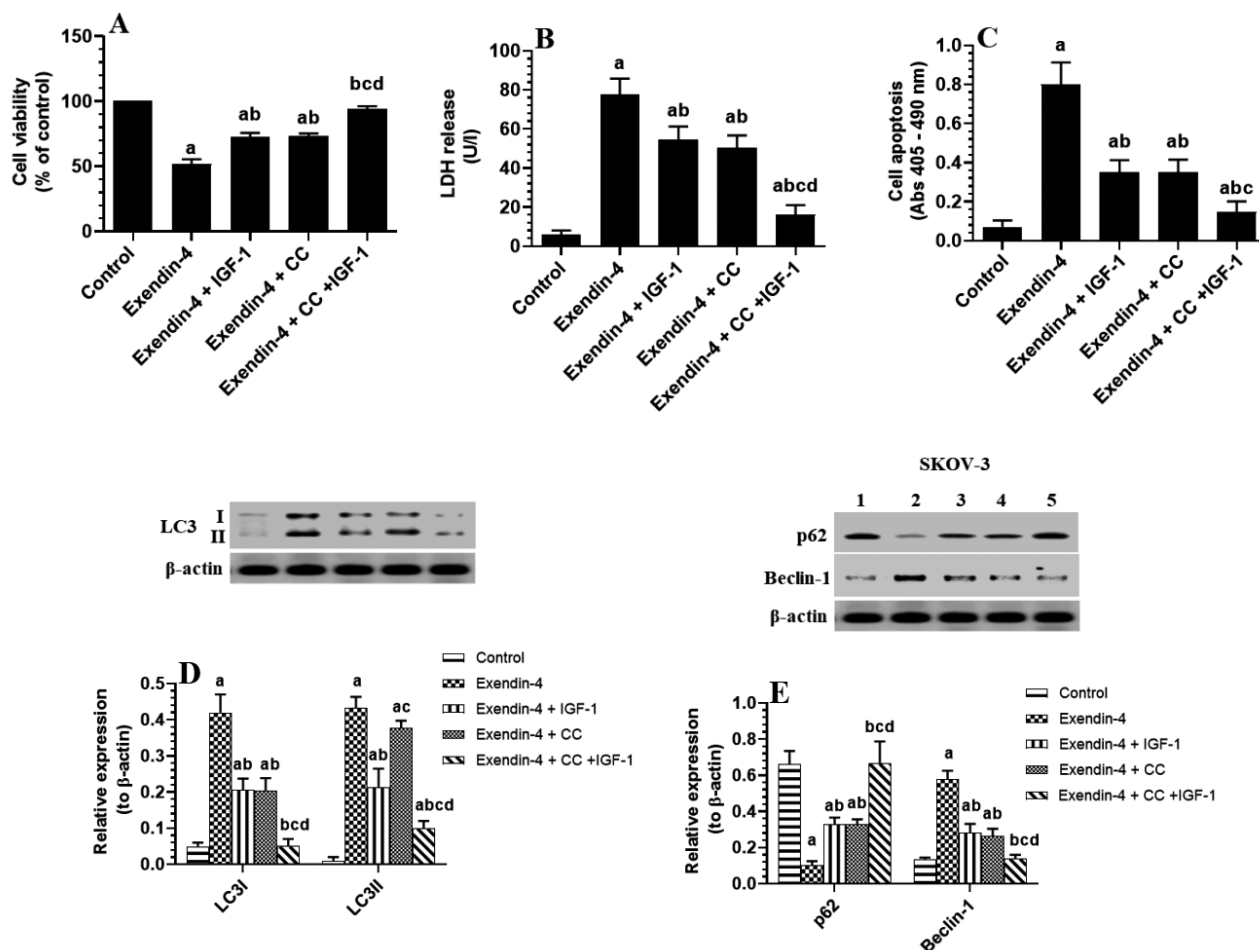


Fig. 9. A combination of insulin-like growth factor-1 (IGF-1), a PI3K/Akt activator, and compound C (CC), a selective AMPK inhibitor, completely prevents the inhibitory effect of exendin-4 on cell survival and its stimulation of apoptosis and LDH release in the treated SKOV-3 cells. Cells were cultured at a density of $1 \times 10^5/\text{ml}$ in DMEM medium for 24 h and treated with exendin-4 (30 μM for SKOV-3). Control cells were treated with 0.1% DMSO. Data are presented as mean \pm SD. ^a Significantly different as compared to control cells. ^b Significantly different as compared to exendin-4-treated cells.

Discussion

GLP-1 and its receptor agonist, exendin-4, are widely used for the treatment of T2DM because of their potent glucose-lowering, augmenting post-prandial insulin secretion, inhibiting glucagon secretion, promoting β -cell proliferation, inducing satiety, and delaying gastric emptying effects (Park et al., 2007). However, GLP-1Rs are widely distributed in numerous cells and organs including the liver, hypothalamus, pancreas, kidney, heart, endothelial cells, neurons, glial cells, and immune cells (Iwai et al., 2006; Park et al., 2007; Arakawa et al., 2010; Romani-Pérez et al., 2013; Pyke et al., 2014; Heppner et al., 2015). Currently, the protective anti-oxidant, anti-inflammatory, and anti-apoptotic effects of exendin-4 have been established in several organs such as the pancreas, kidney, liver, heart under various stress conditions, where exendin-4 modulated several and different signalling pathways (Ferdaoussi et al., 2008; Kim et al., 2012; Wei et al., 2012; Chen et al., 2013; Zhou et al.,

2014; Eid et al., 2020a,b). However, opposing this, the pro-apoptotic role of exendin-4 and other GLP-1R agonists has been reported in solid tumours including breast, prostate and ovarian cancer (Vangoitsenhoven et al., 2012; Nomiya et al., 2014; Tsutsumi et al., 2015; He et al., 2016; Zhang et al., 2016; Iwaya et al., 2017; Khaleel et al., 2020).

On the other hand, the sustained use of GLP-1 is associated with a higher risk of developing thyroid cancer (Vangoitsenhoven et al., 2012). Until now, such antagonizing anti-apoptotic and apoptotic effects of exendin-4 have remained largely unknown. However, it seems reasonable that the cell fate effect of exendin-4 depends on several factors including tissue factors such as tissue metabolic activity, environment (pH), cell density, and GLP-1R receptor density.

Supporting its tumour-suppressive effect, the finding of this study also confirmed that exogenous exendin-4 exerts a tumour-suppressor effect in the two tested OC

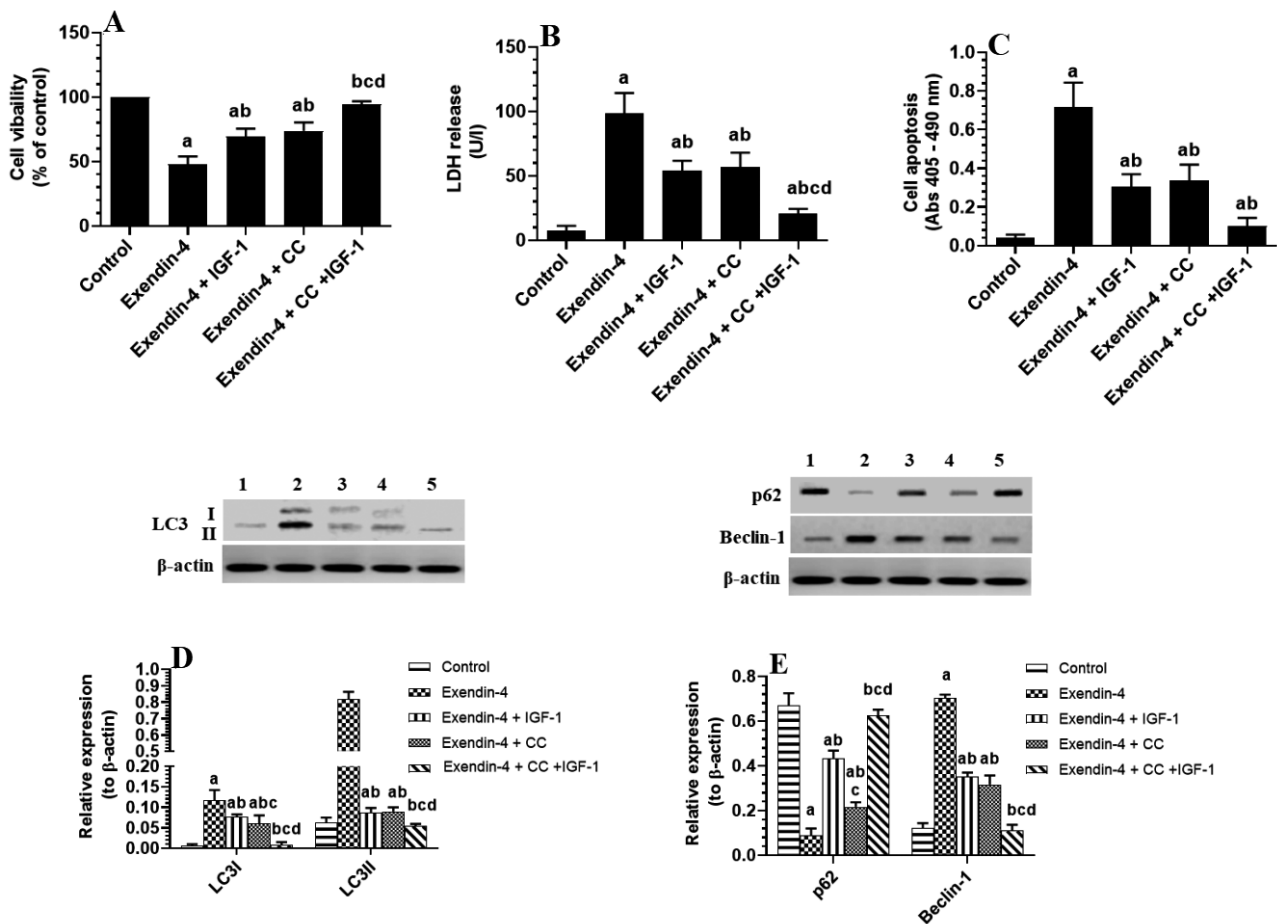


Fig. 10. A combination of insulin-like growth factor-1 (IGF-1), a PI3K/Akt activator, and compound C (CC), a selective AMPK inhibitor, completely prevents the inhibitory effect of exendin-4 on cell survival and its stimulation of apoptosis and LDH release in the treated OVCAR-3 cells. Cells were cultured at a density of 1×10^5 /ml in DMEM medium for 24 h and treated with exendin-4 (40 μ M for OVCAR-3). Control cells were treated with 0.1% DMSO. Data are presented as mean \pm SD. ^a Significantly different as compared to control cells. ^b Significantly different as compared to exendin-4-treated cells.

cell lines, SKOV-3 and OVCAR-3. Exendin-4 inhibited cell proliferation, reduced survival and induced cell apoptosis, and reduced cell migration and invasion in both cell lines. However, the salient findings of this study are that these anti-tumour effects of exendin-4 in both cell lines were highly dependent on the inhibition of mTORC1 and activation of markers of autophagy (beclin-1 and LC3II) and associated with inhibition of PI3K/Akt and activation of AMPK signalling pathways.

Autophagy plays a significant role in the development/prevention of OC. In OC, autophagy is usually down-regulated, which implies that autophagy harmed cancer cell development and proliferation (Zhan et al., 2016). The autophagy-cytotoxic effect involves up-regulation of apoptosis (Mariño et al., 2014). Of note, lower levels of beclin-1 and LC3II concomitant up-regulation of p62 are associated with the advanced stages of OC, poor prognosis, and low survival rates (Shen et al., 2008; Liu and Ryan, 2012; Lu et al., 2014; Shuvayeva et al., 2014; Zhan et al., 2016). Beclin-1 is involved in the

initiation stage of autophagy, while LC3II is included in the elongation stage and formation of the autophagosome (Cai et al., 2014). p62 acts as an adaptor protein that links LC3II with the ubiquitin moieties on misfolded proteins (Bjørkøy et al., 2005; Pankiv et al., 2007). Hence, autophagy ensures the clearance of p62 along with the misfolded protein (Zhan et al., 2015). The level of LC3II expression represents the autophagy level in the cell and the up-regulation of beclin-1 and LC3II and suppression of p62 are classical markers of autophagy activation (Zhan et al., 2016).

In this study, exendin-4 increased the cell apoptosis rate, enhanced the release of LDH, suppressed cell survival, and reduced cell invasiveness in both cell lines. Besides, although no solid evidence of functional autophagy is provided, exendin-4 concomitantly stimulated some markers of autophagy in both SKOV-3 and OVCAR-3 cell lines, as indicated by the increased protein levels of beclin-1 and LC3II and the parallel decrease in the expression of p62 in both cell lines. These

data imply that exendin-4 can stimulate autophagy, and such activation of autophagy could be a protective cytotoxic means. Indeed, exendin-4 suppressed cell survival and increased cell apoptosis in OC cell lines (He et al., 2016; Khaleel et al., 2020). Several authors have shown that exendin-4 can stimulate autophagy in the brains of diabetic rats, palmitate-treated β -cells, and livers of induced steatosis in mice (Sharma et al., 2011; Zummo et al., 2017; Candeias et al., 2018). Also, exendin-4 prevented cell proliferation and growth of HepG2 cells by activating autophagy (Krause et al., 2019).

Interestingly, reports indicated that p62 triggers DNA damage and persistent activation of nuclear factor κ B (NF- κ B) and nuclear factor erythroid 2-related factor-2 (Nrf-2), two pro-inflammatory and anti-oxidant transcription factors, respectively, that are known to be up-regulated in solid tumours (Duran et al., 2008; Inami et al., 2011). Over-activation of NF- κ B and Nrf-2 plays an essential role in promoting OC cell survival, migration, and invasion (Macciò and Madeddu, 2012; van der Wijst et al., 2014). Nrf-2 promotes OC progression by increasing the expression of numerous endogenous anti-oxidants including anti-oxidant enzymes and GSH (Czogalla et al., 2019). However, NF- κ B stimulates cell survival by increasing expression of several apoptotic inhibitor proteins (AIPs), cell cycle proteins, and Bcl-2 anti-apoptotic-related proteins and blocks activation of multiple caspases (Wu et al., 2009; Macciò and Madeddu, 2012; Xia et al., 2014). Therefore, higher levels of p62 during autophagy suppression such as in OC augments inflammation and increases cellular anti-oxidants, both of which promote OC cell tumorigenesis.

In this study, associated with the reduction in p62, exendin-4 also suppressed the activation of NF- κ B, lowered the expression of Bcl-2, reduced the levels of GSH, and increased the expression of Bax and cleaved caspases 3 and 8 in both the SKOV-3 and OVCAR-3 cell lines. These data suggest that exendin-4-induced cell death in both OC cell lines involves inhibition of cell inflammation, reduction of cyto-protective anti-oxidant activity, and up-regulation of p62, possibly through activating autophagy. These data also imply that the autophagy response that is observed in exendin-4 represents a cytotoxic signal.

Hence, it was of our interest to investigate the role of these autophagy markers in exendin-4-induced cell apoptosis in both cell lines. For this reason, we pre-treated the exendin-4-treated cells with autophagy inhibitor CQ. Generally, CQ inhibits the latest step in autophagy, which is the fusion of the autophagosome and the lysosome (Mauthe et al., 2018). Interestingly, and in both SKOV-3 and OVCAR-3 cell lines, CQ completely abrogated the inhibitory effect afforded by exendin-4 on cancer cell survival, migration, and invasion and abolished exendin-induced apoptosis. Also, CQ completely prevented exendin-4-induced up-regulation of Bax and cleaved caspases 3 and 8 and increased the expression levels of p-NF- κ B (Ser⁵³⁶) and Bcl-2 and the levels of GSH. Based on these data, we became very confident that the

exendin-4 tumour suppressor effects in both cell lines involve suppression of GSH levels and NF- κ B in an autophagy-dependent manner. Recently, our group has demonstrated that the exendin-4 cytotoxic effect in OC cell lines was partially dependent on exendin-4-mediated activation of SIRT1 and subsequent inhibition of NF- κ B (Khaleel et al., 2020). In the same study, we have also shown that exendin-4 altered the expression of several apoptosis-related NF- κ B responsive genes including MMP-9, ICAM-1, Bcl-2, Bax, and cyclin D. Based on our data from this study and our previous report, we could suggest that the anti-tumorigenic effect of exendin-4 in both SKOV-3 and OVCAR-3 cell lines involves autophagy-induced suppression of p62 and activation of SIRT1.

Nonetheless, the activation of autophagy arms is a novel strategy to inhibit OC progression. Various pharmacological agents such as dasatinib, dihydroxytychanol 2, C2-ceramide, MORAB-003, suberoylanilide hydroxamic acid, resveratrol, and rographolide were found to prevent OC through up-regulation of beclin-1, LC3II, and ATGs and inhibition of p62 (reviewed in Zhan et al., 2016). Interestingly, ghrelin, another intestinal hormone, inhibited growth of HO-8910 cells by inducing autophagy. Like the effect shown by exendin-4 in this study, the ghrelin anti-tumour effects included up-regulation of LC3II, beclin-1, and Atg12-Atg5 complex and concomitant down-regulation of p62 (Xu et al., 2013).

Next, we were interested in finding the possible mechanisms by which exendin-4 activated these autophagy markers in both tested OC cell lines. mTOR, a serine/threonine kinase, is an essential cellular nutrient sensor that regulates cell growth and division in response to growth factors, glucose, amino acids, energy status, and different types of stress (Zoncu et al., 2011). The mTOR pathway involves two functional complexes: mTOR complexes 1 and 2 (mTORC1 and mTORC2), both of which are activated in response to IGF-1-induced activation of PI3K/Akt (Ravikumar et al., 2010). mTORC1 is a potent autophagy inhibitor in normal and cancer cells, including OC (Wei et al., 2018). The pro-oncogenic properties of mTORC1 are well studied and were shown to be mediated by increasing the expression and translation of several oncogenes, activation of glycolytic transcription factors and enzymes, and stimulating lipid and purine synthesis, which are needed for cancer cell growth (LoPiccolo et al., 2008; Lien et al., 2016; Liu et al., 2018; Tian et al., 2019). mTORC1 is frequently activated in epithelial OC and has been identified as a novel target for therapy (Mabuchi et al., 2011). Inhibition of mTORC1 kinase activity decreases phosphorylation of two downstream target effectors: ribosomal protein S6 kinase 1 (S6K1) at Thr³⁸⁹/Thr⁴²¹/Ser⁴²⁴ and translation initiation factor 4E-binding protein (4E-BP1) at Thr³⁷/Thr⁴⁶ (LoPiccolo et al., 2008; Zoncu et al., 2011; Tian et al., 2019).

The activity of mTORC1 is mainly regulated by two upstream regulators, Akt and AMPK, which stimulate or inhibit mTORC1, respectively (Zhan et al., 2016). A de-

tailed description of mTOR signalling and its relation to autophagy can be found in excellent reviews (Ravikumar et al., 2010). In general, lower activation of AMPK and sustained activation of PI3K/Akt are well reported in multiple types of cancers including OC cells and were correlated with their development, progression, metastasis, invasion, and advanced stages through activation of mTORC1 (Luo et al., 2010; Mabuchi et al., 2011; Yung et al., 2016; Tian et al., 2019).

In this study, we provide evidence that the increase in levels of beclin-1 and LC3II after exendin-4 treatment in both SKOV-3 and OVCAR-3 cells is due to the inhibition of mTORC1 mediated by suppression of Akt and activation of AMPK. Indeed, associated with the higher expression levels of autophagy markers, cell apoptosis, and inhibition of cell migration, exendin-4 also suppressed mTOR activation, reduced phosphorylation of S6K1 and 4E-BP-1, two downstream targets of mTOR, inhibited Akt activation, and increased AMPK activity in both SKOV-3 and OVCAR-3 cells. To precisely determine the contribution of each of these pathways in the observed effect of exendin-4 on the autophagy markers, we pre-treated the exendin-4-treated cells with IGF-1, a PI3K/Akt/mTORC1 activator, or with CC, an AMPK inhibitor, either individually or in combination. As expected, the use of IGF-1 or CC as a solo treatment partially prevented exendin-4 inhibitory effects on the cell survival, invasion, and migration. They also partially reduced exendin-4-induced activation of beclin-1, LC3I/II, and the increase in p62. Notably, combined treatment with both IGF-1 and CC in exendin-4-treated cells completely prevented all these effects afforded by exendin-4. Based on these findings, we have concluded that the activation of AMPK and concurrent inhibition of PI3K/Akt is required for the cytotoxic autophagy induced by exendin-4. These data support the study of He et al., who have shown that exendin-4 inhibits cell proliferation, migration, and invasion of a variety of OC cells including SKOV-3, OVCAR-3, OVCAR-4, A2780, and ES-2 by inhibiting PI3K/Akt (He et al., 2016). However, our study also suggests that this effect also involves the activation of AMPK.

Despite these data, this study has some limitations. First of all, the doses of exendin-4 used in this study (30 and 40 μ M) are much higher than those reported by other authors in OC cell lines or other types of cancer (in nM). We have previously run a dose-response experiment on both cell lines to determine the IC_{50} of exendin-4 that corresponds to each cell line. We have shown that such higher doses are required to inhibit the cell survival of both the SKOV-3 and OVCAR-3 cells by 50 %. Such variation in the effective dose has also been reported by other authors using the same cell lines. For example, while Ligumsky et al. (2012) have shown that exendin-4 at doses of 50 nM can inhibit growth and proliferation of MCF-7 breast cancer cell lines, Fidan-Yaylılı et al. (2016) have demonstrated that higher doses (5–10 μ M) are needed to produce similar effects in the same cell lines. Therefore, such variation between

our data and those of others could be explained by the variation in several undetermined factors including the source of the cells, stage of the disease, age of the cells, density of GLP-1R, experimental conditions, and the source and activity of exendin-4. At this stage, we could not further figure out the source of variation, which needs further investigation. Besides, although these data suggest the involvement of autophagy in the protective effect of exendin-4, no solid evidence for functional autophagy is provided. Therefore, more advanced studies are required to confirm this effect. Furthermore, the effect afforded by exendin-4 on these cells could be through unidentified receptors, an effect that was not confirmed in this study. The lack of the use of GLP-1R agonists in this study adds more limitations and should be further investigated in the upcoming studies.

In conclusion, this study is the first to shed light on the role of autophagy in the anti-tumour effect of exendin-4 in OC. The data presented here suggest that the anti-tumour effect afforded by exendin-4 in both SKOV-3 and OVCAR-3 cell lines is associated with an anti-inflammatory effect and up-regulation of autophagy. These effects are mediated by suppressing mTORC1 with concurrent activation of AMPK and inhibition of PI3K/Akt signalling pathways.

Conflict of interest

The authors declare no conflict of interest.

Acknowledgements

The authors wish to thank the technical staff at the animal house facilities, College of Medicine, King Khalid university (KKU). The authors also pass their gratitude to the technical staff at the departments of Biochemistry, Physiology and Pathology, College of Medicine, KKU for their assistance.

References

- Arakawa, M., Mita, T., Azuma, K., Ebato, C., Goto, H., Nomiya, T., Fujitani, Y., Hirose, T., Kawamori, R., Watada, H. (2010) Inhibition of monocyte adhesion to endothelial cells and attenuation of atherosclerotic lesion by a glucagon-like peptide-1 receptor agonist, exendin-4. *Diabetes* **59**, 1030-1037.
- Bai, H., Li, H., Li, W., Gui, T., Yang, J., Cao, D., Shen, K. (2015) The PI3K/AKT/mTOR pathway is a potential predictor of distinct invasive and migratory capacities in human ovarian cancer cell lines. *Oncotarget* **6**, 25520-25532.
- Bao, L., Jaramillo, M. C., Zhang, Z., Zheng, Y., Yao, M., Zhang, D. D., Yi, X. (2015) Induction of autophagy contributes to cisplatin resistance in human ovarian cancer cells. *Mol. Med. Rep.* **11**, 91-98.
- Bjørkøy, G., Lamark, T., Brech, A., Outzen, H., Perander, M., Øvervatn, A., Stenmark, H., Johansen, T. (2005) p62/SQSTM1 forms protein aggregates degraded by autophagy and has a protective effect on huntingtin-induced cell death. *J. Cell Biol.* **171**, 603-614.
- Cai, M., Hu, Z., Liu, J., Gao, J., Liu, C., Liu, D., Tan, M., Zhang, D., Lin, B. (2014) Beclin 1 expression in ovarian

- tissues and its effects on ovarian cancer prognosis. *Int. J. Mol. Sci.* **15**, 5292-5303.
- Candeias, E., Sebastião, I., Cardoso, S., Carvalho, C., Santos, M. S., Oliveira, C. R., Moreira, P. I., Duarte, A. I. (2018) Brain GLP-1/IGF-1 signaling and autophagy mediate exendin-4 protection against apoptosis in type 2 diabetic rats. *Mol. Neurobiol.* **55**, 4030-4050.
- Chen, Y. T., Tsai, T. H., Yang, C. C., Sun, C. K., Chang, L. T., Chen, H. H., Chang, C. L., Sung, P. H., Zhen, Y. Y., Leu, S., Chang, H. W., Chen, Y. L., Yip, H. K. (2013) Exendin-4 and sitagliptin protect kidney from ischemia-reperfusion injury through suppressing oxidative stress and inflammatory reaction. *J. Transl. Med.* **11**, 270
- Correa, R. J. M., Valdes, Y. R., Shepherd, T. G., DiMattia, G. E. (2015) Beclin-1 expression is retained in high-grade serous ovarian cancer yet is not essential for autophagy induction in vitro. *J. Ovarian Res.* **8**, 52.
- Czogalla, B., Kahaly, M., Mayr, D., Schmoekel, E., Niesler, B., Kolben, T., Burges, A., Mahner, S., Jeschke, U., Trillsch, F. (2019) Interaction of ER α and NRF2 impacts survival in ovarian cancer patients. *Int. J. Mol. Sci.* **20**, 112.
- Ding, Z., Liu, S., Wang, X., Dai, Y., Khaidakov, M., Romeo, F., Mehta, J. L. (2014) LOX-1, oxidant stress, mtDNA damage, autophagy, and immune response in atherosclerosis. *Can. J. Physiol. Pharmacol.* **92**, 524-530
- Duran, A., Linares, J. F., Galvez, A. S., Wikenheiser, K., Flores, J. M., Diaz-Meco, M. T., Moscat, J. (2008) The signaling adaptor p62 is an important NF- κ B mediator in tumorigenesis. *Cancer Cell* **13**, 343-354.
- Eid, R. A., Bin-Meferij, M. M., El-kott, A. F., Eleawa, S. M., Zaki, M. S. A., Al-Shraim, M., El-Sayed, F., Eldeen, M. A., Alkhateeb, M. A., Alharbi, S. A., Aldera, H., Khalil, M. A. (2020a) Exendin-4 protects against myocardial ischemia-reperfusion injury by upregulation of SIRT1 and SIRT3 and activation of AMPK. *J. Cardiovasc. Transl. Res.* Epub ahead of print. PMID: 32239434, DOI: 10.1007/s12265-020-09984-5.
- Eid, R. A., Khalil, M. A., Alkhateeb, M. A., Eleawa, S. M., Zaki, M. S. A., El-kott, A. F., Al-Shraim, M., El-Sayed, F., Eldeen, M. A., Bin-Meferij, M. M., Awaji, K. M. E., Shatoor, A. S. (2020b) Exendin-4 attenuates remodeling in the remote myocardium of rats after an acute myocardial infarction by activating β -arrestin-2, protein phosphatase 2A, and glycogen synthase kinase-3 and inhibiting β -catenin. *Cardiovasc. Drugs Ther.* Epub ahead of print. PMID: 32474680.
- Ferdaoussi, M., Abdelli, S., Yang, J. Y., Cornu, M., Niederhauser, G., Favre, D., Widmann, C., Regazzi, R., Thorens, B., Waeber, G., Abderrahmani, A. (2008) Exendin-4 protects β -cells from interleukin-1 β -induced apoptosis by interfering with the c-Jun NH2-terminal kinase pathway. *Diabetes* **57**, 1205-1215.
- Fidan-Yaylı, G., Dodurga, Y., Seçme, M., Elmas, L. (2016) Antidiabetic exendin-4 activates apoptotic pathway and inhibits growth of breast cancer cells. *Tumor Biol.* **37**, 2647-2653.
- He, W., Yu, S., Wang, L., He, M., Cao, X., Li, Y., Xiao, H. (2016) Exendin-4 inhibits growth and augments apoptosis of ovarian cancer cells. *Mol. Cell. Endocrinol.* **436**, 240-249.
- Heppner, K. M., Kirigiti, M., Secher, A., Paulsen, S. J., Buckingham, R., Pyke, C., Knudsen, L. B., Vrang, N., Grove, K. L. (2015) Expression and distribution of glucagon-like peptide-1 receptor mRNA, protein and binding in the male nonhuman primate (*Macaca mulatta*) brain. *Endocrinology* **156**, 255-267.
- Holst, J. J. (2007) The physiology of glucagon-like peptide 1. *Physiol. Rev.* **87**, 1409-1439.
- Inami, Y., Waguri, S., Sakamoto, A., Kouno, T., Nakada, K., Hino, O., Watanabe, S., Ando, J., Iwadate, M., Yamamoto, M., Lee, M. S., Tanaka, K., Komatsu, M. (2011) Persistent activation of Nrf2 through p62 in hepatocellular carcinoma cells. *J. Cell Biol.* **193**, 275-284.
- Iwai, T., Ito, S., Tanimitsu, K., Udagawa, S., Oka, J. I. (2006) Glucagon-like peptide-1 inhibits LPS-induced IL-1 β production in cultured rat astrocytes. *Neurosci. Res.* **55**, 352-360.
- Iwaya, C., Nomiyama, T., Komatsu, S., Kawanami, T., Tsutsumi, Y., Hamaguchi, Y., Horikawa, T., Yoshinaga, Y., Yamashita, S., Tanaka, T., Terawaki, Y., Tanabe, M., Nabeshima, K., Iwasaki, A., Yanase, T. (2017) Exendin-4, a glucagonlike peptide-1 receptor agonist, attenuates breast cancer growth by inhibiting NF- κ B activation. *Endocrinology* **158**, 4218-4232.
- Khaleel, E. F., Badi, R. M., Satti, H. H., Mostafa, D. G. (2020) Exendin-4 exhibits a tumour suppressor effect in SKOVR-3 and OVACR-3 ovarian cancer cells lines by the activation of SIRT1 and inhibition of NF- κ B. *Clin. Exp. Pharmacol. Physiol.* **47**, 1092-1102.
- Kim, J. Y., Lim, D. M., Park, H. S., Moon, C. I., Choi, K. J., Lee, S. K., Baik, H. W., Park, K. Y., Kim, B. J. (2012) Exendin-4 protects against sulfonylurea-induced β -cell apoptosis. *J. Pharmacol. Sci.* **118**, 65-74.
- Krause, G. C., Lima, K. G., Levorse, V., Haute, G. V., Gassen, R. B., Garcia, M. C., Pedrazza, L., Donadio, M. V. F., Luft, C., Oliveira, J. R. (2019) Exenatide induces autophagy and prevents the cell regrowth in HEPG2 cells. *EXCLI J.* **18**, 540-548.
- Lien, E. C., Lyssiotis, C. A., Cantley, L. C. (2016) Metabolic reprogramming by the PI3K-Akt-mTOR pathway in cancer. In: *Recent Results in Cancer Research*. Springer New York LLC, pp. 39-72.
- Ligumsky, H., Wolf, I., Israeli, S., Haimsohn, M., Ferber, S., Karasik, A., Kaufman, B., Rubinek, T. (2012) The peptide-hormone glucagon-like peptide-1 activates cAMP and inhibits growth of breast cancer cells. *Breast Cancer Res. Treat.* **132**, 449-461.
- Liu, E. Y., Ryan, K. M. (2012) Autophagy and cancer – issues we need to digest. *J. Cell Sci.* **125**, 2349-2358.
- Liu, Y., Tong, L., Luo, Y., Li, X., Chen, G., Wang, Y. (2018) Resveratrol inhibits the proliferation and induces the apoptosis in ovarian cancer cells via inhibiting glycolysis and targeting AMPK/mTOR signaling pathway. *J. Cell. Biochem.* **119**, 6162–6172.
- LoPiccolo, J., Blumenthal, G. M., Bernstein, W. B., Dennis, P. A. (2008) Targeting the PI3K/Akt/mTOR pathway: effective combinations and clinical considerations. *Drug Resist. Updat.* **11**, 32-50.
- Lu, Z., Yang, H., Sutton, M. N., Yang, M., Clarke, C. H., Liao, W. S. L., Bast, R. C. (2014) ARHI (DIRAS3) induces autophagy in ovarian cancer cells by downregulating the epidermal growth factor receptor, inhibiting PI3K and Ras/

- MAP signaling and activating the FOXo3a-mediated induction of Rab7. *Cell Death Differ.* **21**, 1275-1289.
- Luo, Z., Zang, M., Guo, W. (2010) AMPK as a metabolic tumor suppressor: control of metabolism and cell growth. *Futur. Oncol.* **6**, 457-470.
- Mabuchi, S., Hisamatsu, T., Kimura, T. (2011) Targeting mTOR signaling pathway in ovarian cancer. *Curr. Med. Chem.* **18**, 2960-2968.
- Macciò, A., Madeddu, C. (2012) Inflammation and ovarian cancer. *Cytokine* **58**, 133-1487.
- Manic, G., Obrist, F., Kroemer, G., Vitale, I., Galluzzi, L. (2014) Chloroquine and hydroxychloroquine for cancer therapy. *Mol. Cell. Oncol.* **1**, e29911.
- Mariño, G., Niso-Santano, M., Baehrecke, E. H., Kroemer, G. (2014) Self-consumption: the interplay of autophagy and apoptosis. *Nat. Rev. Mol. Cell Biol.* **15**, 81-94.
- Mauthe, M., Orhon, I., Rocchi, C., Zhou, X., Luhr, M., Hijlkema, K. J., Coppes, R. P., Engedal, N., Mari, M., Reggiori, F. (2018) Chloroquine inhibits autophagic flux by decreasing autophagosome-lysosome fusion. *Autophagy* **14**, 1435-1455.
- Mizushima, N., Levine, B., Cuervo, A. M., Klionsky, D. J. (2008) Autophagy fights disease through cellular self-digestion. *Nature* **451**, 1069-1075.
- Morgan, S. L., Medina, J. E., Taylor, M. M., Dinulescu, D. M. (2014) Targeting platinum resistant disease in ovarian cancer. *Curr. Med. Chem.* **21**, 3009-3020.
- Nomiyama, T., Kawanami, T., Irie, S., Hamaguchi, Y., Terawaki, Y., Murase, K., Tsutsumi, Y., Nagaishi, R., Tanabe, M., Morinaga, H., Tanaka, T., Mizoguchi, M., Nabeshima, K., Tanaka, M., Yanase, T. (2014) Exendin-4, a GLP-1 receptor agonist, attenuates prostate cancer growth. *Diabetes* **63**, 3891-3905.
- Pankiv, S., Clausen, T. H., Lamark, T., Brech, A., Bruun, J. A., Outzen, H., Øvervatn, A., Bjørkøy, G., Johansen, T. (2007) p62/SQSTM1 binds directly to Atg8/LC3 to facilitate degradation of ubiquitinated protein aggregates by autophagy. *J. Biol. Chem.* **282**, 24131-24145.
- Park, C. W., Kim, H. W., Ko, S. H., Lim, J. H., Ryu, G. R., Chung, H. W., Han, S. W., Shin, S. J., Bang, B. K., Breyer, M. D., Chang, Y. S. (2007) Long-term treatment of glucagon-like peptide-1 analog exendin-4 ameliorates diabetic nephropathy through improving metabolic anomalies in db/db mice. *J. Am. Soc. Nephrol.* **18**, 1227-1238.
- Peracchio, C., Alabiso, O., Valente, G., Isidoro, C. (2012) Involvement of autophagy in ovarian cancer: a working hypothesis. *J. Ovarian Res.* **5**, 22.
- Pyke, C., Heller, R. S., Kirk, R. K., Ørskov, C., Reedtz-Runge, S., Kaastrup, P., Hvelplund, A., Bardram, L., Calatayud, D., Knudsen, L. B. (2014) GLP-1 receptor localization in monkey and human tissue: novel distribution revealed with extensively validated monoclonal antibody. *Endocrinology* **155**, 1280-1290.
- Ravikumar, B., Sarkar, S., Davies, J. E., Futter, M., Garcia-Arencibia, M., Green-Thompson, Z. W., Jimenez-Sanchez, M., Korolchuk, V. I., Lichtenberg, M., Luo, S., Massey, D. C. O., Menzies, F. M., Moreau, K., Narayanan, U., Renna, M., Siddiqi, F. H., Underwood, B. R., Winslow, A. R., Rubinsztein, D. C. (2010) Regulation of mammalian autophagy in physiology and pathophysiology. *Physiol. Rev.* **90**, 1383-1435.
- Romani-Pérez, M., Outeiriño-Iglesias, V., Gil-Lozano, M., González-Matías, L. C., Mallo, F., Vigo, E. (2013) Pulmonary GLP-1 receptor increases at birth and exogenous GLP-1 receptor agonists augmented surfactant-protein levels in litters from normal and nitrofen-treated pregnant rats. *Endocrinology* **154**, 1144-1155.
- Sharma, S., Mellis, J. E., Fu, P. P., Saxena, N. K., Anania, F. A. (2011) GLP-1 analogs reduce hepatocyte steatosis and improve survival by enhancing the unfolded protein response and promoting macroautophagy. *PLoS One* **6**, e25269.
- Shen, Y., Li, D. D., Wang, L. L., Deng, R., Zhu, X. F. (2008) Decreased expression of autophagy-related proteins in malignant epithelial ovarian cancer. *Autophagy* **4**, 1067-1068.
- Shuvayeva, G., Bobak, Y., Igumentseva, N., Titone, R., Morani, F., Stasyk, O., Isidoro, C. (2014) Single amino acid arginine deprivation triggers prosurvival autophagic response in ovarian carcinoma SKOV3. *Biomed Res. Int.* **2014**, 505041
- Sun, Y., Liu, J. H., Jin, L., Sui, Y. X., Han, L. L., Huang, Y. (2015) Effect of autophagy-related beclin1 on sensitivity of cisplatin-resistant ovarian cancer cells to chemotherapeutic agents. *Asian Pacific J. Cancer Prev.* **16**, 2785-2791.
- Tan, W. X., Xu, T. M., Zhou, Z. L., Lv, X. J., Liu, J., Zhang, W. J., Cui, M. H. (2019) TRP14 promotes resistance to cisplatin by inducing autophagy in ovarian cancer. *Oncol. Rep.* **42**, 1343-1354.
- Tang, J., Zhu, J., Ye, Y., Liu, Y., He, Y., Zhang, L., Tang, D., Qiao, C., Feng, X., Li, J., Kan, Y., Li, X., Jin, X., Kong, D. (2019) Inhibition LC3B can increase chemosensitivity of ovarian cancer cells. *Cancer Cell Int.* **19**, 199.
- Tian, T., Li, X., Zhang, J. (2019) mTOR signaling in cancer and mTOR inhibitors in solid tumor targeting therapy. *Int. J. Mol. Sci.* **20**, 755.
- Tsutsumi, Y., Nomiyama, T., Kawanami, T., Hamaguchi, Y., Terawaki, Y., Tanaka, T., Murase, K., Motonaga, R., Tanabe, M., Yanase, T., Culig, Z. (2015) Combined treatment with exendin-4 and metformin attenuates prostate cancer growth. *PLoS One* **10**, e0139709
- Van der Wijst, M. G. P., Brown, R., Rots, M. G. (2014) Nrf2, the master redox switch: the Achilles' heel of ovarian cancer? *Biochim. Biophys. Acta Rev. Cancer* **1846**, 494-509.
- Vangoitsenhoven, R., Mathieu, C., Van Der Schueren, B. (2012) GLP1 and cancer: friend or foe? *Endocr. Relat. Cancer* **19**, F77-F88.
- Vaughan, S., Coward, J. I., Bast, R. C., Berchuck, A., Berek, J. S., Brenton, J. D., Coukos, G., Crum, C. C., Drapkin, R., Etemadmoghadam, D., Friedlander, M., Gabra, H., Kaye, S. B., Lord, C. J., Lengyel, E., Levine, D. A., McNeish, I. A., Menon, U., Mills, G. B., Nephew, K. P., Oza, A. M., Sood, A. K., Stronach, E. A., Walczak, H., Bowtell, D. D., Balkwill, F. R. (2011) Rethinking ovarian cancer: recommendations for improving outcomes. *Nat. Rev. Cancer* **11**, 719-725.
- Vijayakumar, K., Cho, G. (2019) Autophagy: an evolutionarily conserved process in the maintenance of stem cells and aging. *Cell Biochem. Funct.* **37**, 452-458.

- Wei, Q., Sun, Y. Q., Zhang, J. (2012) Exendin-4, a glucagon-like peptide-1 receptor agonist, inhibits cell apoptosis induced by lipotoxicity in pancreatic β -cell line. *Peptides* **37**, 18-24.
- Wei, Y., Han, T., Wang, R., Wei, J., Peng, K., Lin, Q., Shao, G. (2018) LSD1 negatively regulates autophagy through the mTOR signaling pathway in ovarian cancer cells. *Oncol. Rep.* **40**, 425-433.
- Wu, Y., Deng, J., Rychahou, P. G., Qiu, S., Evers, B. M., Zhou, B. P. (2009) Stabilization of Snail by NF- κ B is required for inflammation-induced cell migration and invasion. *Cancer Cell* **15**, 416-428.
- Xia, Y., Shen, S., Verma, I. M. (2014) NF- κ B, an active player in human cancers. *Cancer Immunol. Res.* **2**, 823-830.
- Xu, Y., Pang, X., Dong, M., Wen, F., Zhang, Y. (2013) Ghrelin inhibits ovarian epithelial carcinoma cell proliferation in vitro. *Oncol. Rep.* **30**, 2063-2070.
- Yap, M. K. K., Misuan, N. (2019) Exendin-4 from *Heloderma suspectum* venom: from discovery to its latest application as type II diabetes combatant. *Basic Clin. Pharmacol. Toxicol.* **124**, 513-527.
- Ylä-Anttila, P., Vihinen, H., Jokitalo, E., Eskelinen, E.-L. (2009) 3D tomography reveals connections between the phagophore and endoplasmic reticulum. *Autophagy* **5**, 1180-1185.
- Yun, C. W., Lee, S. H. (2018) The roles of autophagy in cancer. *Int. J. Mol. Sci.* **19**, 3466.
- Yung, M. M. H., Ngan, H. Y. S., Chan, D. W. (2016) Targeting AMPK signaling in combating ovarian cancers: opportunities and challenges. *Acta Biochim. Biophys. Sin. (Shanghai)* **48**, 301-317.
- Zhan, L., Yang, Y., Ma, T. T., Huang, C., Meng, X. M., Zhang, L., Li, J. (2015) Transient receptor potential vanilloid 4 inhibits rat HSC-T6 apoptosis through induction of autophagy. *Mol. Cell. Biochem.* **402**, 9-22.
- Zhan, L., Zhang, Y., Wang, W., Song, E., Fan, Y., Li, J., Wei, B. (2016) Autophagy as an emerging therapy target for ovarian carcinoma. *Oncotarget* **7**, 83476-83487.
- Zhang, Y., Xu, F., Liang, H., Cai, M., Wen, X., Li, X., Weng, J. (2016) Exenatide inhibits the growth of endometrial cancer Ishikawa xenografts in nude mice. *Oncol. Rep.* **35**, 1340-1348.
- Zhou, H., Yang, J., Xin, T., Li, D., Guo, J., Hu, S., Zhou, S., Zhang, T., Zhang, Y., Han, T., Chen, Y. (2014) Exendin-4 protects adipose-derived mesenchymal stem cells from apoptosis induced by hydrogen peroxide through the PI3K/Akt-Sfrp2 pathways. *Free Radic. Biol. Med.* **77**, 363-375.
- Zi, D., Zhou, Z. W., Yang, Y. J., Huang, L., Zhou, Z. L., He, S. M., He, Z. X., Zhou, S. F. (2015) Danusertib induces apoptosis, cell cycle arrest, and autophagy but inhibits epithelial to mesenchymal transition involving PI3K/Akt/mTOR signaling pathway in human ovarian cancer cells. *Int. J. Mol. Sci.* **16**, 27228-27251.
- Zoncu, R., Efeyan, A., Sabatini, D. M. (2011) mTOR: from growth signal integration to cancer, diabetes and ageing. *Nat. Rev. Mol. Cell Biol.* **12**, 21-35.
- Zummo, F. P., Cullen, K. S., Honkanen-Scott, M., Shaw, J. A. M., Lovat, P. E., Arden, A. C. (2017) Glucagon-like peptide 1 protects pancreatic β -cells from death by increasing autophagic flux and restoring lysosomal function. *Diabetes* **66**, 1272-1285.